AGU ADVANCING EARTH AND SPACE SCIENCE

Water Resources Research

RESEARCH ARTICLE
10.1029/2021WR029692

A Framework for Assessing Concentration-Discharge Catchment Behavior From Low-Frequency Water Quality Data

Ina Pohle[1], Nikki Baggaley[1], Javier Palarea-Albaladejo[2,3], Marc Stutter[1,4], and Miriam Glendell[1]

[1]Environmental and Biochemical Sciences Group, The James Hutton Institute, Scotland, UK, [2]Biomathematics and Statistics Scotland, JCMB, Scotland, UK, [3]Department of Computer Science, Applied Mathematics and Statistics, University of Girona, Girona, Spain, [4]Lancaster Environment Centre, Lancaster University, Bailrigg, UK

Key Points:

- A reproducible classification of concentration-discharge relationships was developed
- Export regime and hysteresis pattern of low-frequency water quality data are considered
- Catchment concentration-discharge classification varies spatially and among solutes

Supporting Information:

Supporting Information may be found in the online version of this article.

Correspondence to:

I. Pohle,
Ina.Pohle@hutton.ac.uk;
Ina.Pohle@gmail.com

Citation:

Pohle, I., Baggaley, N., Palarea-Albaladejo, J., Stutter, M., & Glendell, M. (2021). A framework for assessing concentration-discharge catchment behavior from low-frequency water quality data. *Water Resources Research*, *57*, e2021WR029692. https://doi.org/10.1029/2021WR029692

Received 24 JAN 2021
Accepted 13 AUG 2021

Abstract Effective nutrient pollution mitigation measures require in-depth understanding of spatio-temporal controls on water quality which can be obtained by analyzing export regime and hysteresis patterns in concentration-discharge ($c - Q$) relationships. Such analyses require high-frequency data (hourly or higher resolution), hampering the assessment of hysteresis patterns in widely available low-frequency (monthly, biweekly) regulatory water quality data. We propose a reproducible classification of $c - Q$ relationships considering export regime (dilution, constancy, enrichment) and long-term average hysteresis pattern (clockwise, no hysteresis, anticlockwise) applicable to low-frequency water quality data. The classification is based on power-law $c - Q$ models with separate parametrization for low and high discharge and rising and falling hydrograph limb, enabling a better representation of $c - Q$ dynamics. The classification has been applied to a 30-years record of daily streamflow and monthly spot samples of solute concentrations in 45 Scottish catchments with contrasting characteristics in terms of topography, climate, soil and land cover. We found that $c - Q$ classification is solute- and catchment-specific and linked to upland versus lowland catchments and streamflow variability. However as the relationship between solute behavior and catchment characteristics is variable, we propose that future typologies should integrate both water quality response, that is, $c - Q$ classification, and catchment characteristics. The data-driven $c - Q$ classification allows us to increase the information content of low-frequency water quality data and thus inform mitigation measures, monitoring strategies, and modeling approaches. Such approaches open up an ability to characterize processes and best management for a wider number of catchments, subject to regulatory surveillance and outside of research catchments.

1. Introduction

Instream water quality is highly variable in space and time (Guo et al., 2019; Lintern et al., 2018) as it represents the integrated response to hydrological and biogeochemical processes in a catchment (Arheimer & Lidén, 2000; Miller et al., 2017). Understanding spatial and temporal controls on solute sources and pathways is required to plan effective mitigation measures (Bieroza et al., 2018; Bowes et al., 2014) and to estimate impacts of environmental changes (Bol et al., 2018; Krause et al., 2014). Spatial controls on solute exports include extent and distribution of solute sources, water available for transport and hydrological connectivity and hence relate to land cover, climate, topography, and soil (e.g., Bracken et al., 2013; Lintern et al., 2018; Reddy et al., 1999). Temporal controls on solute export include hydrometeorological variables such as rainfall (Aguilera & Melack, 2018) and snowmelt (Rosenberg & Schroth, 2017), intermittent sources (Causse et al., 2015), and riparian (Duncan et al., 2015) and instream (Creed et al., 2015) processes. Due to complex interactions across spatial and temporal scales, various authors reported challenges in identifying dominant controls on instream concentrations, especially in large and heterogeneous catchments (e.g., Ali et al., 2017; Heathwaite et al., 2005; Zhou et al., 2017).

The relationships between concentration and discharge ($c - Q$ relationships) as integrated signals of catchment response are used to investigate spatial and temporal controls on solute exports during individual runoff events (e.g., Aguilera & Melack, 2018; Hunsaker & Johnson, 2017) and for longer time series (e.g., Bieroza & Heathwaite, 2015; Creed & Band, 1998; Winnick et al., 2017). Quantitative comparisons among catchments, solutes, or time periods require describing $c - Q$ relationships by statistical models (Ali

et al., 2017; Minaudo et al., 2019). Typically, power-law models are employed to describe general patterns between concentration and discharge magnitudes:

$$c = a \times Q^b \quad (1)$$

with c as concentration, Q as discharge and a and b as intercept and slope of the power-law models. A positive slope b (enrichment, i.e., concentration increases with discharge), indicates transport-limited mobilization due to large element storage in combination with enhanced mobilization for example, due to increased connectivity. Negative slope (dilution, i.e., concentration decreases with discharge) is attributed to source limitation (Basu et al., 2011). Near-zero slopes (constancy, i.e., no significant changes of concentrations with discharge) indicate homogeneous element distribution, invariant source areas or synchronous hydrological and biogeochemical processes (Li et al., 2017; Moatar et al., 2017; Musolff et al., 2015). Here it should be noted that Thompson et al. (2011) emphasize that near-zero slopes do not necessarily imply small concentration variability as concentrations might vary independently from discharge. Further, general patterns between concentration and discharge magnitude may be obscured by various influences, including seasonal and long-term variations (Minaudo et al., 2019).

Hysteresis in $c - Q$ relationships is analyzed to investigate time lags between discharge and concentration (Dupas et al., 2016; Lawler et al., 2006) and to identify flow pathways (L. A. Rose et al., 2018). Higher concentrations at the rising compared to the falling limb of the hydrograph (clockwise hysteresis), is interpreted as fast response to runoff events, that is, flushing (Bieroza & Heathwaite, 2015). In contrast, anticlockwise hysteresis may be related to delayed transport processes for example, from upstream parts of the catchment or via subsurface flow. While export regime has been described both for individual events and long-term series of different temporal resolution, hysteresis patterns in $c - Q$ relationships are generally derived from high-frequency, that is, hourly or sub-hourly concentration and discharge data, which are available for few catchments and for a limited number of years (e.g., Bieroza et al., 2018; Duncan et al., 2017).

Another way of analyzing concentrations with respect to discharge is to compare their, for example, by assessing chemostatic and chemodynamic behavior using the ratio between coefficients of variations (Musolff et al., 2015). Chemodynamic behavior, that is, high concentration variability compared to discharge, is interpreted as biogeochemically controlled and non-uniform element distribution in space (Basu et al., 2010). Chemostatic behavior is interpreted as hydrologically controlled with large and homogeneous element stores in the catchment (Basu et al., 2010; Thompson et al., 2011). It should be noted that other authors (e.g., Bieroza et al., 2018; Godsey et al., 2009) define chemostasis based on near-zero slopes of power-law $c - Q$ models rather than coefficients of variation which does not take into account variation in concentration independently from discharge (Thompson et al., 2011). Power-law $c - Q$ slopes and the ratio between coefficients of variations between concentration and discharge are interlinked (Jawitz & Mitchell, 2011) in the sense that low coefficients of variations do not coincide with very high or very low $c - Q$ slopes as also illustrated in Figure 2a of Musolff et al. (2015).

Classification schemes have been developed to analyze and compare $c - Q$ behavior between different locations and/or different time periods. For example, Evans and Davies (1998) classify event responses taking into account hysteresis patterns, curvature (a measure for discharge vs. concentration variability within an event) and export regimes (i.e., general patterns between concentration and discharge magnitude). Vaughan et al. (2017) use a similar approach to classify event responses based on general patterns between concentration and discharge magnitude and hysteresis patterns. Musolff et al. (2017) classify long time series of solute concentrations according to general patterns between discharge and concentration magnitudes as well as concentration versus discharge variability (using the ratio between their coefficients of variations). Moatar et al. (2017) developed a classification applicable to low-resolution water quality data based on distinct $c - Q$ slopes for discharge below and above median discharge. A classification considering both seasonal and event $c - Q$ response has been introduced by Minaudo et al. (2019).

Developing catchment typologies to group catchments according to their solute export behavior is essential for information transfer from data-rich to data-poor catchments (Krause et al., 2014). These typologies can be used as decision support for targeting mitigation measures and for informing monitoring designs and water quality models. Due to the complexity of catchment response to interlinked spatial and temporal controls (Arheimer & Lidén, 2000; Heathwaite et al., 2005; Lintern et al., 2018) deriving typologies a priori based on catchment characteristics such as climate, topography and land cover alone may be challenging.

Hence, catchment behavior groupings may be improved by combining catchment characteristics and waterbody responses, the latter including hydrological (dis)similarities (Sawicz et al., 2011). Both spatial and temporal controls on solute export behavior should be considered when developing catchment typologies in order to better understand how solute exports respond to changes in environmental conditions. A large data resource to evaluate hydrochemical behaviors commonly exists as regulatory surveillance data as decadal time series of low frequency (e.g., monthly). Such data contrast the high temporal resolution, research catchment intra-storm data on which $c - Q$ analysis are generally undertaken in terms of potential for much greater spatial coverage, but providing a composite of inter-storm periods (effectively acting as surrogates for intra-storm samples) plus decadal background change and management influences.

This study describes a data analysis framework developed to facilitate river hydrochemical response analysis on large national data resources. Our hypothesis was that $c - Q$ classification of long-term low-frequency data can identify and group solute export behaviors. The study aimed to contrast more conservative solutes indicative of hydrological controls (calcium Ca, chloride Cl and silicate SiO_2) with reactive solutes (nitrate $NO_3 - N$, ammonia $NH_4 - N$, soluble reactive phosphorus SRP, dissolved organic carbon DOC) and support hydrochemical inferences of catchment groupings with catchment characteristics. The case study presented of Scotland provides contrasting catchment properties (topography, climate, soil, land cover) to maximize hydrochemical behavior differences as a test case expected to strengthen classification differences. The data resource comprised 45 catchments of 30 years of streamflow and water quality data. The classification technique presented in this study can group catchments according to their solute export behavior and thus help support watershed management decisions based on long-term, low-frequency datasets which are widely available for many catchments.

2. Data and Methods

2.1. Classification of $c - Q$ Relationships

In this paper, a classification of $c - Q$ relationships with respect to the general pattern between concentration and discharge magnitudes (export regime) and hysteresis pattern applicable to low-frequency concentrations is proposed. The classification includes categories accounted for by Evans and Davies (1998) considering export regimes (i.e., general patterns between concentration and discharge magnitude) and hysteresis patterns, with advancement regarding applicability to low-frequency data. Export regime distinguishes enrichment (concentration increases with discharge), constancy (no significant relationship between concentration and discharge magnitudes) and dilution (concentration decreases with discharge).

Long-term average hysteresis patterns are considered in terms of clockwise hysteresis, no hysteresis, and anticlockwise hysteresis. The analysis of hysteresis patterns based on low-frequency water quality data (rather than individual runoff events captured with high-frequency data) is based on a discretization of long-term daily discharge time series into rising and falling hydrograph limbs. Clockwise hysteresis characterized by peak concentrations before streamflow peaks is defined in case of higher concentration at the rising limb of the hydrograph. Anticlockwise hysteresis characterized by peak concentration after streamflow peaks is defined in case of higher concentrations at the falling limb of the hydrograph. Insignificant differences between rising and falling limb are considered as no hysteresis.

Considering export regimes and hysteresis patterns, nine types of $c - Q$ relationships are distinguished (Figure 1): enrichment and clockwise (enr, cw), enrichment and no hysteresis (enr, nh), enrichment and anticlockwise (enr, acw), constancy and clockwise (con, cw), constancy and no hysteresis (con, nh), constancy and anticlockwise (con, acw), dilution and clockwise (dil, cw), dilution and no hysteresis (dil, nh), and dilution and anticlockwise (dil, acw). A reproducible classification of $c - Q$ relationships is achieved by utilizing statistical tests to distinguish between export regimes and between hysteresis patterns.

A categorization of $c - Q$ behavior according to the proposed classification requires $c - Q$ models considering discharge magnitude and timing, that is, rising and falling hydrograph limb. Based on the power-law model in Equation 1, separate parameter sets for discharge below and above Q_{50} (discharge with an exceedance frequency of 50%) have been introduced by Meybeck and Moatar (2012). To better represent catchment and substance specific export characteristics, we modified this approach by segmentation at an optimal segmentation discharge Q_{aut} and separate $c - Q$ models for rising and falling hydrograph limb:

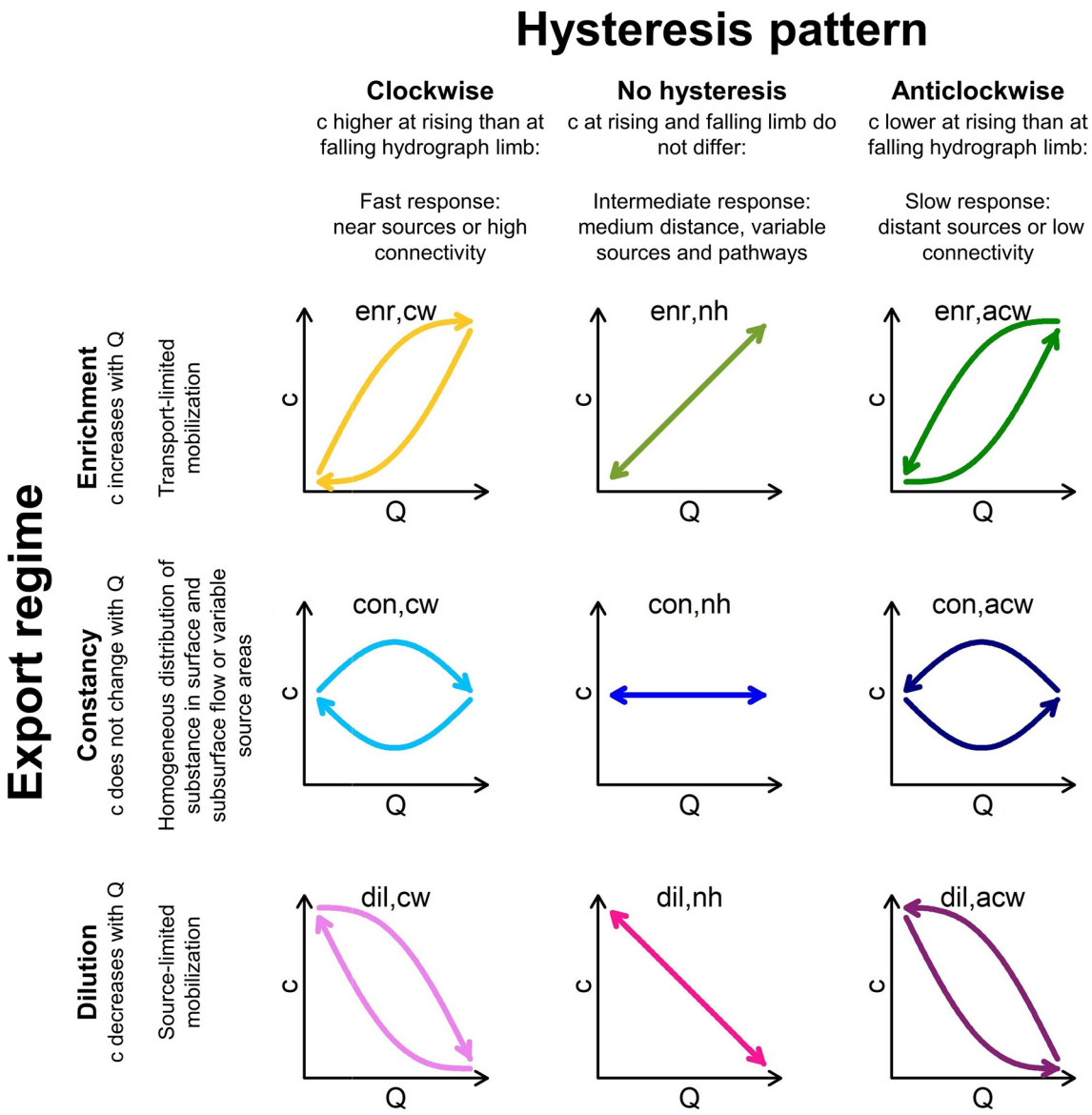

Figure 1. Classification of $c - Q$ relationships based on export regime (enrichment (*enr*), constancy (*con*), dilution (*dil*)), and hysteresis (clockwise (*cw*), none (*nh*), anticlockwise (*acw*)).

$$c = \begin{cases} a_{inf,rise} \times Q^{b_{inf,rise}} & \text{for } Q < Q_{aut,rise} \quad \text{and rising hydrograph} \\ a_{sup,rise} \times Q^{b_{sup,rise}} & \text{for } Q \geq Q_{aut,rise} \quad \text{and rising hydrograph} \\ a_{inf,fall} \times Q^{b_{inf,fall}} & \text{for } Q < Q_{aut,fall} \quad \text{and falling hydrograph} \\ a_{sup,fall} \times Q^{b_{sup,fall}} & \text{for } Q \geq Q_{aut,fall} \quad \text{and falling hydrograph} \end{cases} \tag{2}$$

with (a) $a_{inf,rise}$ and $b_{inf,rise}$ as intercept and slope of the power-law models for rising hydrograph and discharge below the segmentation discharge at the rising hydrograph $Q_{aut,rise}$, (b) $a_{sup,rise}$ and $b_{sup,rise}$ as intercept and slope of the power-law models for rising hydrograph and discharge above $Q_{aut,rise}$, (c) $a_{inf,fall}$ and $b_{inf,fall}$ as intercept and slope of the power-law models for falling hydrograph and discharge below the segmentation discharge at the falling hydrograph $Q_{aut,fall}$, and (d) $a_{sup,fall}$ and $b_{sup,fall}$ as intercept and slope of the power-law models for falling hydrograph and discharge above $Q_{aut,fall}$. For each catchment and substance power-law models were fitted numerically for all combinations of discharge percentiles (1–99) and sep-

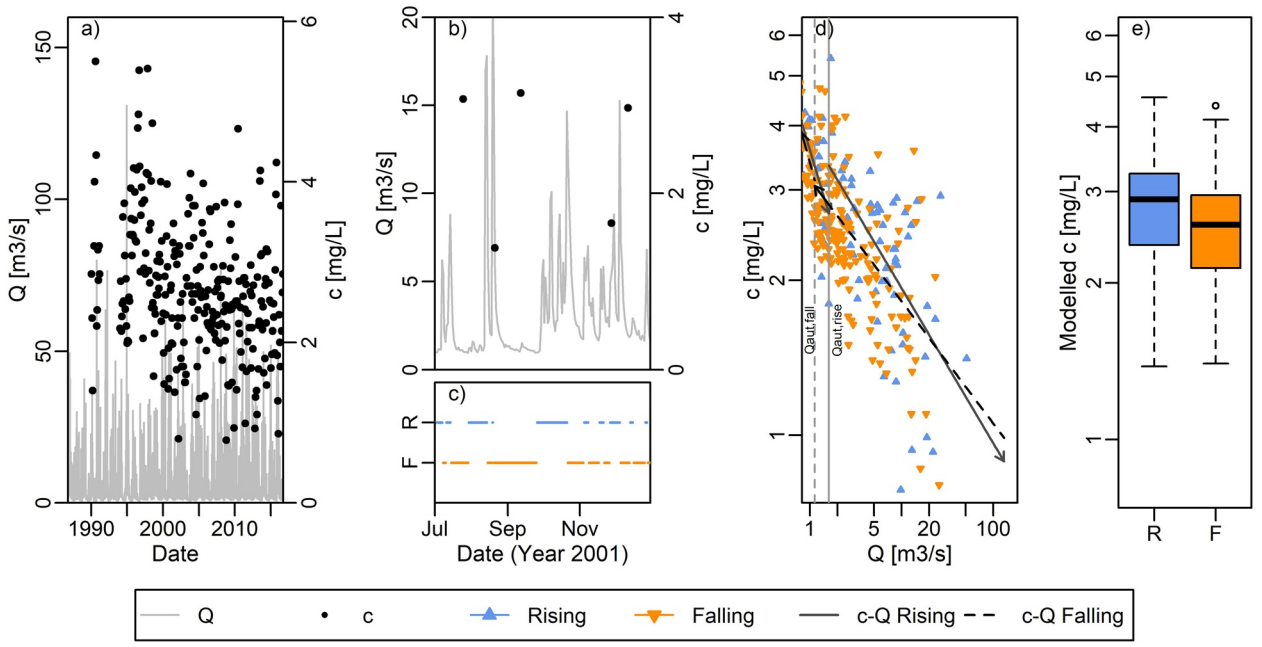

Figure 2. Illustrative example of the classification of $c - Q$ relationships for nitrate concentrations of the River Nairn at Findhall: (a) daily discharge Q and monthly concentrations c, (b) daily discharge (line) and monthly concentrations (points) examplified for July–December 2001. (c) indication of rising (R, blue) and falling (F, orange) hydrograph limbs for the time period shown in sub-figure (b), (d) c versus Q for individual samples for rising (blue) and falling (orange) hydrograph limbs, segmentation discharges for rising ($Q_{aut,rise}$: solid vertical line) and falling hydrograph ($Q_{aut,fall}$: dashed vertical line) limbs as well as fitted $c - Q$ model considering discharge magnitude and hydrograph timing (Equation 2): $Q < Q_{aut,rise}$ and rising hydrograph (solid gray arrow for Q below $Q_{aut,rise}$), $Q \geq Q_{aut,rise}$ and rising hydrograph (solid gray arrow for Q above $Q_{aut,rise}$), $Q < Q_{aut,fall}$ and falling hydrograph (dashed black arrow for Q below $Q_{aut,fall}$), $Q \geq Q_{aut,fall}$ and falling hydrograph (dashed black arrow for Q above $Q_{aut,fall}$). (e) modeled concentrations for all discharge percentiles at rising R and falling F hydrograph limbs.

arately for rising and falling hydrograph limb using the nlsLM function implemented in the R package minpack.lm (Elzhov et al., 2016). The combined power-law equations were applied to model concentrations for all discharge percentiles. The discharge associated with the model with the highest coefficient of determination between modeled and observed concentrations was selected as segmentation discharge Q_{aut}. Runoff events were defined as consecutive time periods when daily discharge exceeded base-flow (using the function baseflows in the R package hydrostats Bond, 2016). The entire time series is classified as either rising or falling whereby the days from lowest discharge between two events up to and including peak event discharge were assigned as rising, the days after peak discharge until the lowest discharge between this event and the next as falling hydrograph limb.

Modeled concentrations (Equation 2) were used to define export regimes and hysteresis patterns. Significant concentration changes with discharge (Mann-Kendall test, p-value ≤ 0.05) and linear slopes between concentration and discharge were analyzed to distinguish increases and decreases of concentration with discharge. Significant concentration increases with discharge at both the rising and falling limb of the hydrograph were categorized as enrichment, consistent significant decreases as dilution. All other cases, that is, insignificant changes or changing directions of $c - Q$ slopes were summarized as constancy. Significant differences between modeled concentrations at rising hydrograph limbs and those at falling hydrograph limbs were assessed by the Kruskal–Wallis test (p-value ≤ 0.05) with clockwise hysteresis classified in cases with higher concentrations at the rising limb, anticlockwise hysteresis in case with higher concentrations at the falling limb, otherwise no hysteresis was assumed. This enabled the analysis of hysteresis of low-frequency data in contrast to analyzing hysteresis loops of individual events of high-frequency data. Modeled rather than observed concentration was chosen to avoid effects of disproportionally many concentration samples at lower discharge and rising limbs, respectively, and better comparability among catchments with differing data availability.

The example in Figure 2 illustrates the sequence of methods to classify $c - Q$ relationships for daily discharge and monthly concentrations of one catchments (Figure 2a). At first, the hydrograph is discretized into rising and falling limb (Figure 2b exemplified for the year 2001). Based on 99 power-law $c - Q$ models for discharge percentiles between 1 and 99, the segmentation discharges $Q_{aut,rise}$ and $Q_{aut,fall}$ and the final $c - Q$ models are derived (Figure 2c). As modeled concentrations significantly decrease with discharge, dilution behavior is determined. The comparison of modeled concentrations for all discharge percentiles further shows higher concentrations at the rising limb than at the falling limb (Figure 2d) indicating clockwise hysteresis so that the $c - Q$ relationship is classified as dilution and clockwise hysteresis (dil, cw).

2.2. Assessment of Chemostatic Versus Chemodynamic Behavior

As a comparative technique to the classification of $c - Q$ relationships, chemostatic versus chemodynamic behavior was assessed by comparing discharge and concentration variability based on the ratio between the coefficient of variation of concentration, CV_c and the coefficient of variation of discharge CV_Q following the definition by Musolff et al. (2017). Hereby, $CV_c/CV_Q > 0.5$ indicates chemodynamic behavior and $CV_c/CV_Q \leq 0.5$ indicates chemostatic behavior. We computed CV_c based on monthly grab sample concentrations and CV_Q based on daily discharge.

2.3. Study Region and Data

We investigated $c - Q$ relationships and catchment similarity in discharge and concentration variability based on mean daily discharge and grab samples of monthly concentration records during the time period 1987–2016 in 45 catchments (area between 55 and 4,587 km^2) covering around 50% of mainland Scotland (Table 1, Figure S2). The catchments are heterogeneous in terms of topographic, climatic, soil, land cover conditions as well as streamflow variability as exemplified for mean altitude, annual precipitation, proportion of peat and organo-mineral soils, and baseflow index BFI in Figure 3.

Long term annual precipitation in the study region ranges from 791 to 2,600 mm (standard reference period 1981–2010, study period 1987–2016: 804–2660 mm) and mean annual air temperature between 5.7°C and 8.7°C (standard reference period 1981–2010, study period 1987–2016: 5.9°C–8.8°C). The climatic characteristics were derived based on the MetOffice UKCP09 data set (Hadley Centre for Climate Prediction and Research, 2017).

Soil characteristics were derived from the Scottish national soil map at 1:250000 scale (Soil Survey of Scotland Staff, 1984). The area of each soil series within the catchments was calculated from the map unit area and corresponding soil series proportions. The soil series were grouped in two ways based on the 11 conceptual models from the Hydrology of Soil Types (HOST) classification (Boorman et al., 1995), first based on the presence and depth of groundwater or aquifer, distinguishing soils with no significant groundwater influence, soils affected by shallow groundwater within 2 m from the land surface, and soils influenced by groundwater deeper than 2 m. Soils were further grouped based on dominant flow pathways within the soil profile, distinguishing soils with prolonged saturated near surface and subsurface lateral flow pathways, soils with some seasonal saturated subsurface lateral flow and soils with predominantly vertical unsaturated flow. Peat (histosols with histic surface horizons ≥50 cm) and organo-mineral soils (soils with histic surface horizons <50 cm depth) were distinguished as a separate class. Peat covers up to 64% of the individual catchments considered in this study and 20% of mainland Scotland in total but contains 40% of the carbon stock to 1 m depth (Baggaley et al., 2016), with significant additional storage to depths greater than 10 m in some areas (Chapman et al., 2009). Three soil categories of cultivation and drainage were considered (artificially drained soils, non-drained cultivated soils and soils not under cultivation. The presence of artificially drained soils was defined based on the occurrence of arable and improved grassland on soils with near-surface gleying (Lilly et al., 2012).

Land cover percentages according to the Land Cover Map LCM2007 (Morton et al., 2011) include woodland (broadleaved and coniferous woodland), semi-natural land (montane habitats, acid grassland, calcareous grassland, neutral grassland, rough grassland, and dwarf and shrub heath), arable land, improved grassland, bogs, freshwater bodies and urban and sub-urban land cover. Other land cover types (supra-littoral rock, supra-littoral sediment, littoral rock, littoral sediment, inland rock, and saltwater) together represent less than 3% of individual catchment areas.

Table 1
Overview of Catchment Characteristics (Details in Tables S11–S13)

Characteristic	Median (range)
Topography	
Area [km^2]	380 (55–4,587)
Mean altitude [m]	230 (80–459)
Maximum altitude [m]	631 (227–1,307)
Slope [%]	9 (3–30)
Soil	
No significant groundwater or aquifer [%]	59 (36–91)
Shallow groundwater [%]	5 (0–24)
Deep groundwater [%]	32 (4–56)
Vertical flow [%]	23 (4–66)
Seasonal saturated flow [%]	10 (0–63)
Prolonged saturated flow [%]	13 (0–81)
Peat and organo-mineral soils [%]	34 (1–88)
Artificially drained soil [%]	16 (0–67)
Non-drained cultivated soil [%]	9 (0–57)
Not cultivated soil [%]	66 (16–99)
Peat [%]	15 (0–71)
Climate (1987–2016)	
Precipitation [mm]	1,364 (804–2660)
Air temperature [$°C$]	7.7 (5.9–8.8)
Land cover	
Woodland [%]	14 (5–56)
Semi-natural land [%]	32 (8–78)
Arable land [%]	6 (0–56)
Improved grassland [%]	18 (1–69)
Bog [%]	4 (0–48)
Freshwater [%]	1 (0–10)
(Sub-)Urban land [%]	1 (0–28)
Hydrology (1987–2016)	
Runoff [mm]	842 (273–2,474)
RBI[]	0.33 (0.07–0.69)
ΔPar[]	1.29 (0.59–1.59)
IR[]	1.48 (0.35–2.85)
BFI[]	0.46 (0.31–0.62)
$nRev$[$year^{-1}$]	134 (105–181)

Note. Topographic, and climatic catchment characteristics, soil and land cover percentages as well as runoff refer to the entire catchment area, hydrological indices (RBI Richards-Baker flashiness index, ΔPar range of Pardé coefficients, IR interquartile ratio, BFI base-flow index, $nRev$ number of hydrograph reversals per year) refer to streamflow at the catchment outlets.

The hydrological variability of the catchments is expressed by mean annual runoff and variability indices computed from daily streamflow in the period 1987–2016. Variability in distribution was assessed by the interquartile ratio IR. Seasonality was described by the range of Pardé coefficients ΔPar introduced by Viglione et al. (2013). Discharge oscillation was described by the Richards–Baker–Index RBI (Baker et al., 2004)

and the number of hydrograph reversals *nRev* per year, that is, the number of times when differences in daily discharge change from positive to negative or vice versa. Base-flow index *BFI* was used to describe streamflow components. The calculation of variability indices is outlined in Supporting Information S1.

Instream concentrations of calcium (*Ca*), chloride (*Cl*), silica (SiO_2), ammonium-nitrogen ($NH_4 - N$), and nitrate-nitrogen ($NO_3 - N$), soluble reactive phosphorous (*SRP*) and dissolved organic carbon (*DOC*) were included in the analysis. Chemical analyses were carried out at accredited laboratories by the Scottish Environment Protection Agency as the national regulator using standard water quality assessment methods after minimal storage times at 4°C. Briefly, major metals were analyzed by ICP (inductively coupled plasma) emission spectroscopy, *DOC* by chemical oxidation and IR detection on filtrates (<0.45 micrometers). $NO_3 - N$, *SRP* (molybdate blue reaction), *Cl*, *Si* and $NH_4 - N$ were determined colorimetrically with filtration only for highly turbid samples (<1 micrometer). On average, data from 300 water quality samples per site have been included (Table S14) so that the concentration observations are representative of discharge variability capturing both low and high flows.

2.4. Associations Between Instream Solute Response and Catchment Characteristics

Climatic conditions (e.g., Guillemot et al., 2020; Musolff et al., 2018), topography (e.g., Sliva & Williams, 2001; Zhou et al., 2017), land cover (e.g., Kändler et al., 2017; Lepistö et al., 2006), soil (e.g., Fischer et al., 2017; Lintern et al., 2018) and streamflow variability (e.g., Deelstra et al., 2014; Mellander et al., 2015) are recognized as catchment controls of solute exports from catchments. Hence, in this study, the catchments were described by several subsets of variables referring to climatic conditions (annual precipitation and mean air temperature in the time period 1987–2016), topography (catchment area, mean and maximum altitude, mean slope), land cover percentages, soil and hydrological indices (mean annual runoff and streamflow indices (*IR*, ΔPar, *RBI*, *nRev*, and *BFI*) based on daily discharge in the time period 1987–2016). Multiple factor analysis (*MFA*) was used to integrate them all into a common space in order to investigate their associations with either $c - Q$ type or chemodynamic versus chemostatic behavior for each solute. *MFA* weighs each subset so that they have equal weights in the global analysis, accounting for different variabilities amongst the sets of variables, to facilitate the overall assessment of similarities and differences between catchments, sets of characteristics and variables within them. As a form of global principal component analysis (*PCA*), the data were projected onto an optimal low-dimensional space for graphical representation on a biplot (e.g., Abdi et al., 2013). *MFA* computations were based on the *R* package *FactoMineR* (Le et al., 2008). The first two *MFA* dimensions, accounting for most of the data variability, were used to produce a consensus biplot diagram including variables and catchments simultaneously. To facilitate the interpretation, this biplot was split into variables and catchments allowing for visual exploration of common structures and discrepancies. The associations between catchment characteristics and solute responses (each treated as an individual data set) were quantified using the *RV* coefficient (Robert & Escoufier, 1976), defined in [0,1] from lowest to highest association. Pairwise *RV* coefficients between data sets were arranged in matrix form and represented visually. The types of $c - Q$ relationships and, in a separate analysis, also chemostatic versus chemodynamic behavior were considered as nominal variables. After checking the distributions of the individual variables the numerical catchment characteristics were generally log-transformed and standardized to accommodate heterogeneous scales of measurement. For land cover percentages a centered log-ratio transformation was applied in accordance to their compositional nature (Pawlowsky-Glahn & Buccianti, 2011). A few zero values in both land cover and soil percentages (0.95% and 1.41% of the cases, respectively) prevented from data transformation and were imputed by estimated small values using the *lrEM* algorithm based on information from the covariance structure (Palarea-Albaladejo & Martín-Fernández, 2015).

3. Results

3.1. Classification of $c - Q$ Relationships

The segmentation discharges $Q_{aut,rise}$ and $Q_{aut,fall}$ of the fitted $c - Q$ relationships according to Equation 2 vary among solutes and catchments (Figure S4). For SiO_2 these percentiles are centered around the median of discharge, whereas for example, for *Ca* the segmentation discharge is higher and for *Cl* lower than median discharge. The complex $c - Q$ models according to Equation 2 perform better than simple power-law

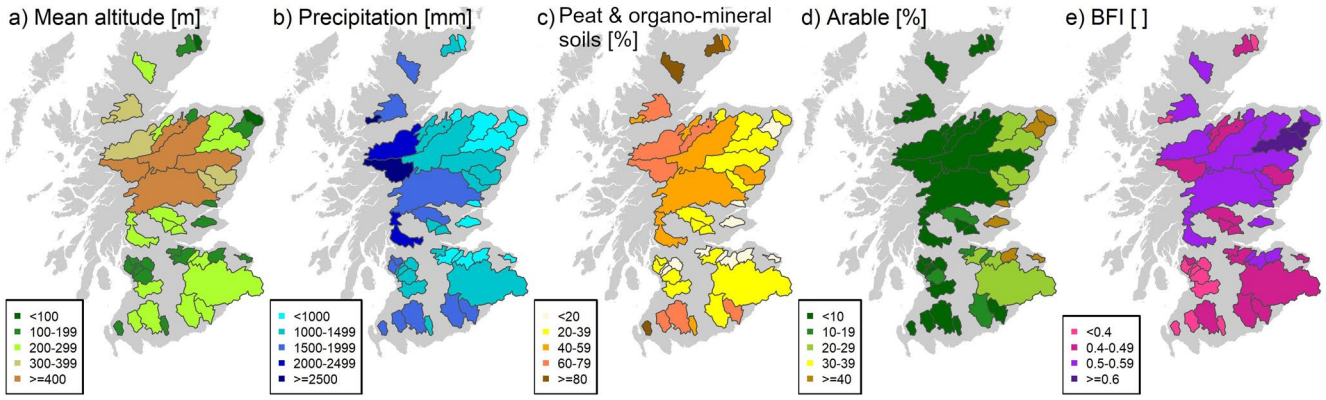

Figure 3. Spatial distribution of (a) mean catchment altitude, (b) mean annual precipitation (1987–2016), (c) proportion of peat and organo-mineral soils, (d) proportion of arable land cover and (e) baseflow index *BFI* (1987–2016). Medians and ranges of further catchment characteristics are given in Table 1.

models according to Equation 1 as shown by higher coefficients of determination between observed and modeled concentrations (Figure S5).

All $c-Q$ types exist in Scottish catchments with high variation among catchments and solutes (Figure 4). *Ca* shows dilution in all catchments except one where constancy occurs (Figure 4a)and more often clockwise (*dil*,*cw*: 18 catchments) and no hysteresis (*dil*,*nh*, 21 catchments) than anticlockwise hysteresis (*dil*,*acw*: 4 catchments). For *Cl* all $c-Q$ types occur with a dominance of dilution (28 catchments) and clockwise hysteresis (30 catchments, 19 catchments classified as *dil*,*cw*, Figure 4b). Enrichment of *Cl* tends to occur in small catchments near the coast. SiO_2 shows mostly enrichment (27 catchments) with constancy (15 catchments) either in Northern or in South Western Scotland (Figure 4c). NH_4-N exhibits a high heterogeneity of export regimes (enrichment and constancy in 16 catchments each, dilution in 13 catchments, Figure 4d). Clockwise hysteresis dominates (22 catchments, *con*,*cw* in 10 catchments), followed by no hysteresis (16 catchments). The $c-Q$ types of NO_3-N are very heterogeneous with a dominance of anticlockwise hysteresis (27 catchments, *enr*,*acw* in 16 catchments, Figure 4e). *SRP* displays more often clockwise (27 catchments) than other hysteresis behaviors (Figure 4f) with *dil*,*cw* occurring in 16 mostly small catchments in Central Scotland. *DOC* displays either enrichment (27 catchments) or constancy (9 catchments) with no obvious dominance of hysteresis patterns (Figure 4g). The $c-Q$ classification does not show pronounced similarities among solutes and no homogenization with catchment size, that is, $c-Q$ patterns vary strongly both in small and in large catchments and there is no tendency toward a particular export regime or hysteresis pattern in larger catchments (Figure 4h).

3.2. Assessment of Chemostatic Versus Chemodynamic Behavior

Most of the solutes show a clear dominance of either chemostatic (i.e., $CV_c/CV_Q \leq 0.5$) or chemodynamic (i.e., $CV_c/CV_Q > 0.5$) behavior (Figure 5). Chemostatic behavior prevails for *Ca*, *Cl*, and SiO_2 (more than 39 of the 45 catchments, Figures 5a–5c). The few catchments which show chemodynamic behavior generally differ between these solutes. Also NO_3-N and *DOC* display mainly chemostatic behavior (29 and 32 catchments, respectively, Figures 5e and 5g) and agree in 22 catchments (both chemostatic: 19, both chemodynamic: 3). Chemodynamic behavior dominates for NH_4-N and *SRP* (41 and 43 catchments, Figures 5d and 5f), there is no overlap in catchments showing chemostatic behavior for these solutes. The strong heterogeneity in chemodynamic versus chemostatic behavior among solutes is summarized in Figure 5h which also shows that there is little effect of catchment size. There is no pronounced overlap between $c-Q$ types and chemostatic versus chemodynamic behavior (compare Figure 4 and Figure 5), that is, for the solutes considered chemostatic behavior does not strongly coincide with one particular $c-Q$ type, export regime or hysteresis pattern (also see Figure S10).

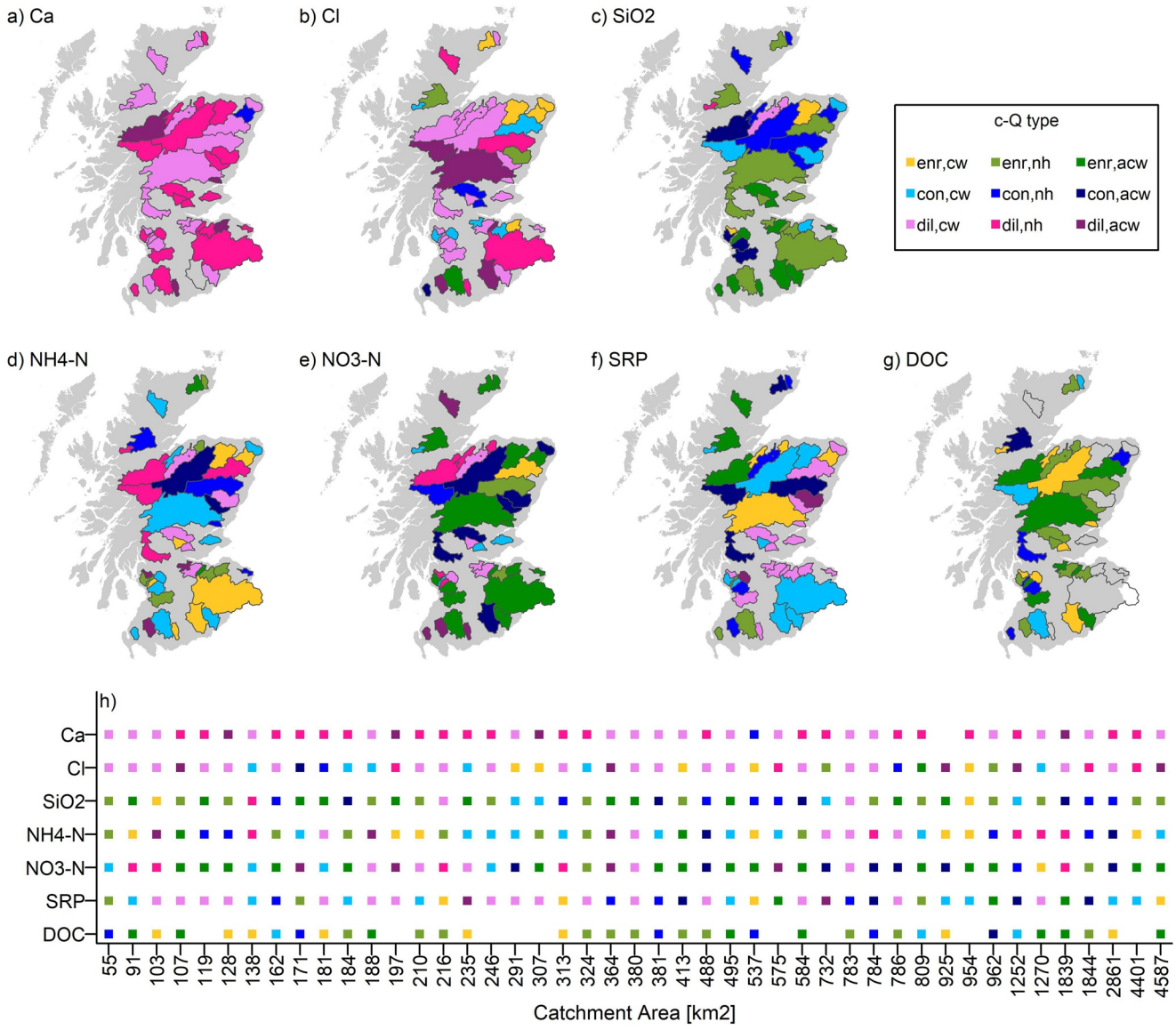

Figure 4. $c-Q$ classification of solutes in Scottish catchments according to Figure 1 considering export regime (enrichment *enr*, constancy *con*, and dilution *dil*) and hysteresis (clockwise *cw*, no hysteresis *nh*, anticlockwise *acw*): (a) *Ca*, (b) *Cl*, (c) SiO_2, (d) NH_4-N, (e) NO_3-N, (f) *SRP*, (g) *DOC*, and (h) $c-Q$ types sorted by increasing catchment area. Due to limited data availability for *Ca* and *DOC* $c-Q$ models according to Equation 2 could not be fitted and $c-Q$ types could not be classified for a few catchments.

3.3. Associations Between Instream Solute Response and Catchment Characteristics

Upland versus lowland catchments and hydrological response appear as important characteristics influencing $c-Q$ classification of all solutes according to the first and second *MFA* axes (*MFA*1 and *MFA*2 respectively; 27.13% total variation explained, Figure 6a, Table S15). Upland catchments (high altitude (*Alt*, *Altx*) and slope (*Slop*), high proportion of woodland (*Wood*), semi-natural land (*Semi*), non-cultivated soil (*NC*), peat soil (*Peat*)) are associated with positive values on the first axis of the *MFA*. Contrastingly lowland catchments (relatively high mean air temperature (*Temp*), high proportion of arable land (*Arbl*), urban and suburban land (*Urb*), grassland (*Gras*)) have negative values on the first axis of the *MFA*. High stream-flow variability (high *RBI*, *IR*, ΔPar (*dPar*)) is related to positive values on the second axis of the *MFA* and low stream-flow variability (high *BFI*) to negative values on this axis. Climatic and soil characteristics are represented by both axes, for example, high precipitation (*Prec*) and high percentage of peat (*Peat*) are

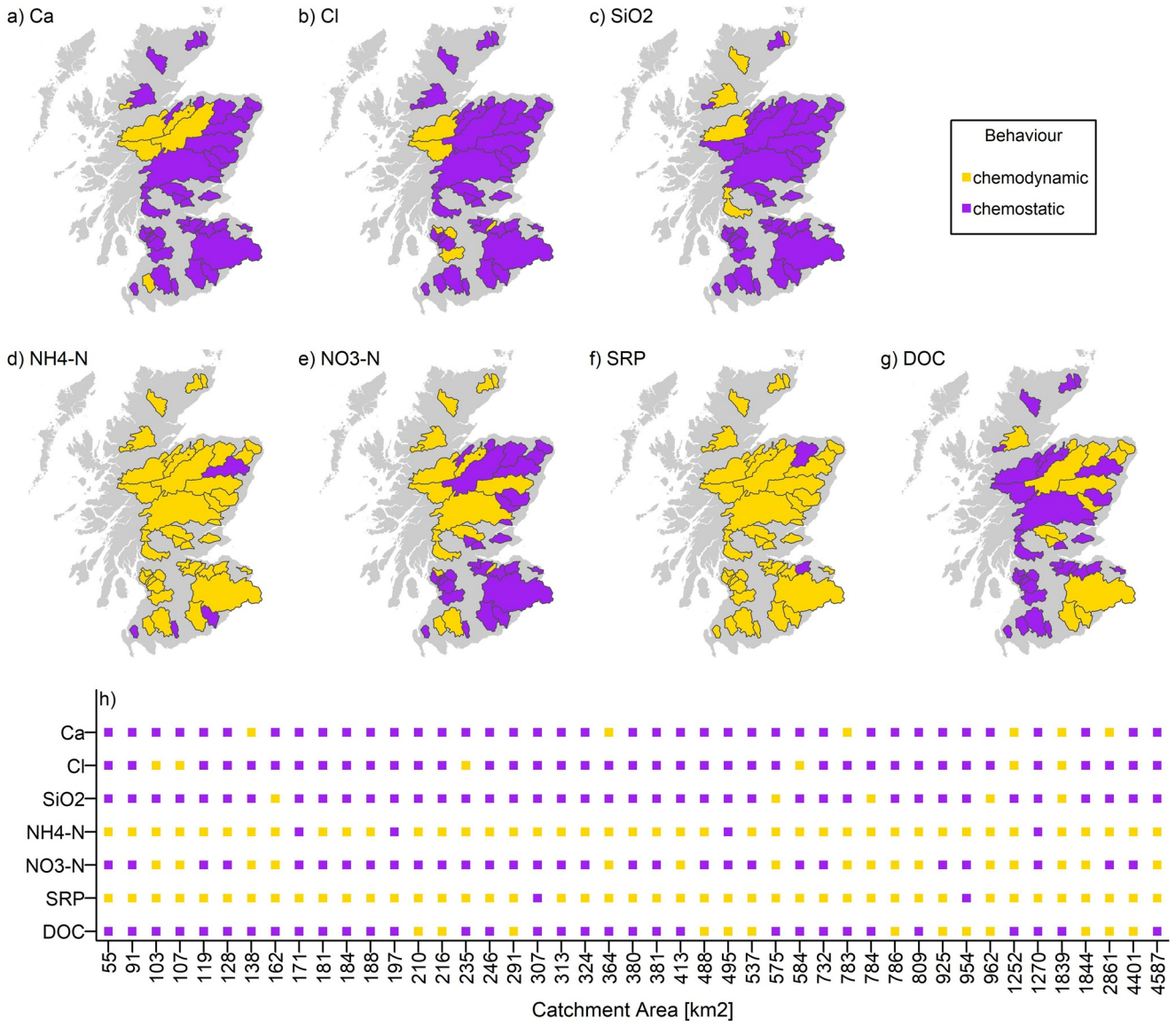

Figure 5. Chemostatic vs. chemodynamic behavior of solutes in Scottish catchments: (a) Ca, (b) Cl, (c) SiO_2, (d) $NH_4 - N$, (e) $NO_3 - N$, (f) SRP, (g) DOC, and (h) chemostatic versus chemodynamic behavior sorted by increasing catchment area.

positively loaded on both *MFA* axes. Predominantly vertical flow (*Vert*) is represented mainly on the second axis with negative values, seasonal lateral flow (*LatS*) is positive on the first and negative on the second axis, whereas prolonged lateral flow (*LatP*) is negative on the first and positive on the second axis. High streamflow variability (positive values on the second *MFA* axis) is linked with dilution of $NO_3 - N$ as shown in Figure 6b by the *MFA* plot for $c - Q$ classification of $NO_3 - N$ (note that a similar position in Figures 6a and 6b indicates a close link with catchment characteristics. The behavior of further solutes is shown in the Figure S6 and demonstrates the solute-specific relationships between individual solute behavior and catchment characteristics. For example, lowland catchments (negative values on the first *MFA* axis) are associated with dilution of *SRP* (Figure S6e). In terms of soil, for example, catchments with a high proportion of artificial drainage are associated with dilution and fast response (mainly *dil*, *cw*) of *SRP* (Figure S6e).

Chemostatic versus chemodynamic behavior also relate to upland versus lowland catchments and hydrological response according to the first two axes of the *MFA* which explain 50.28% of the total variation (Figure 6d, Table S15). Upland catchments are associated with chemodynamic behavior of $NO_3 - N$ (Figure 6e),

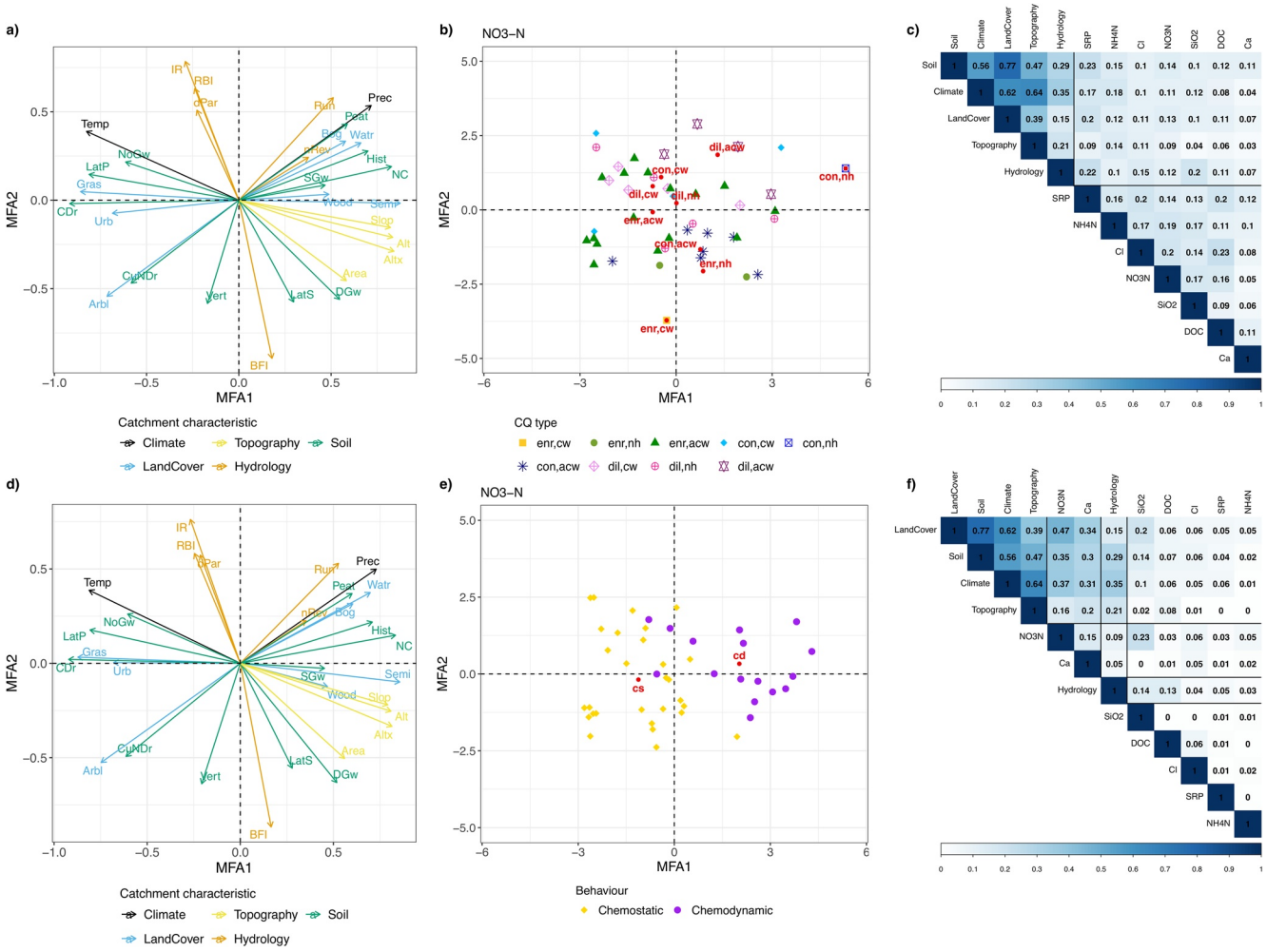

Figure 6. Associations of catchment characteristics with $c-Q$ classification (top row: a–c) and chemostatic versus chemodynamic behavior (bottom row: d–f): (a) *MFA* plot of catchment characteristics associated with $c-Q$ types, (b) *MFA* plot illustrative for $c-Q$ types of NO_3-N showing individual catchments and centroids of the $c-Q$ types as red dots with text (see Figure S6 for other solutes), (c) *RV* coefficients between $c-Q$ types and catchment characteristics (note that the columns are ordered according to overall *RV* values of data sets, i.e., higher to lower from left to right; color intensity represents the strength of the association; black lines are used to separate catchment characteristics and solute response datasets), (d) *MFA* plot of catchment characteristics associated with chemodynamic versus chemostatic behavior, (e) *MFA* plot illustrative for chemostatic versus chemodynamic behavior of NO_3-N (see Figure S7 for other solutes), (f) RV coefficients between chemodynamic versus chemostatic behavior and catchment characteristics. Catchment characteristics: climate (mean annual temperature *Temp*, mean annual precipitation *Prec*), topography (catchment area *Area*, mean altitude *Alt*, maximum altitude *Altx*, mean slope *Slop*), soil (no significant groundwater *NoGW*, shallow groundwater *SGw*, deep groundwater *DGw*, prolonged lateral flow *LatP*, seasonal lateral flow *LatS*, vertical unsaturated flow *Vert*, peat and organo-mineral soils *Hist*, artificially drained soils *CDr*, non-drained cultivated soils *CuNDr*, soils not under cultivation *NC*, *Peat*), land cover (woodland *Wood*, semi-natural *Semi*, arable *Arbl*, improved grassland *Gras*, *Bog*, freshwater bodies *Watr*, (sub)-urban *Urb*), hydrology (runoff *Run*, ΔPar (*dPar*), *RBI*, *nRev*, *IR*, *BFI*). For variance explained by the first two *MFA* axes the reader is referred to the Supporting Information, Table S15.

Ca, SiO_2 and *SRP* (Figures S7a, S7c and S7e). High streamflow variability is, for example, associated with chemodynamic behavior of *Cl* and *SRP* (Figures S7c and S7e).

Catchment characteristics differ in their importance for $c-Q$ classification and chemodynamic versus chemostatic behavior of the individual solutes according to the *MFA* . Associations among catchment characteristics are pronounced, as visible from the close proximity between rays in Figure 6a and high *RV* values, especially between soil and land cover, climate and land cover, and climate and topography (Figures 6c and 6d).

4. Discussion

4.1. Analysis of $c - Q$ Response Based on Low-Frequency Data Can Identify and Group Solute Export Behavior

All $c - Q$ types of our proposed classification (Figure 1) developed to analyze river hydrochemical response using long-term low frequency data can be found in the 45 Scottish study catchments (Figure 4). Following our hypothesis we showed that $c - Q$ response of long-term low-frequency data can identify and group solute export behaviors. Specifically, strong variations among solutes and catchments show that long-term low-frequency national data contain relevant information for such assessments. Solute specific behavior relates to different sources and transport mechanisms while the heterogeneity in $c - Q$ responses relates to gradients in landscape characteristics (topography, climate, soil, and land cover) and contrasts with studies using long-term, low-frequency data in French catchments that reported solute specific dominance of export regimes (Minaudo et al., 2019; Moatar et al., 2017). Further, the Scottish catchments are relatively unpolluted, resulting in a greater sensitivity and range of responses to hydrometeorological drivers. Chemodynamic versus chemostatic behavior show more solute specific responses, with mostly chemostatic behavior for *Ca*, *Cl* and *Si*, mostly chemodynamic behavior for $NH_4 - N$ and *SRP* and catchment-specific responses for $NO_3 - N$ and *DOC*. Upland versus lowland catchments and streamflow variability influence both $c - Q$ classification and chemodynamic versus chemostatic behavior.

Inconsistent $c - Q$ patterns and differences in chemodynamic versus chemostatic behavior (Figures 4, 5, 6c and 6f) among solutes can be indicative of different sources including predominantly diffuse sources of $NO_3 - N$ and *DOC* and point sources, for example, septic tanks, for *SRP* (Richards et al., 2016). Further, different transport pathways and instream processing lead to different response times between runoff events and concentrations at the catchment outlets. For example, $NO_3 - N$ and *DOC* are mobilized more homogeneously from the entire catchment leading to relatively slow responses to events and thus rarely to clockwise hysteresis. Contrastingly, critical source areas with high connectivity to streams play a significant role for *SRP* exports (Hewett et al., 2004; Sharpley et al., 2009), apparent in the fast response to runoff events and predominantly clockwise hysteresis (Figure 4).

We did not find a homogenization of $c - Q$ classification with catchment size (Figure 4h), that is, no tendency toward particular $c - Q$ types, export regimes or hysteresis patterns in larger catchments likely due to contrasting landscape drivers interacting and obscuring any potential size effects. Further, even the smaller catchments in our study are relatively large compared to those in studies investigating smaller headwater catchments (Abbott et al., 2018; Hashemi et al., 2020; Herndon et al., 2015). Some studies found large catchment size to be related to chemostasis (Creed et al., 2015) or chemodynamics (Diamond & Cohen, 2018). In our study, larger catchments tend toward chemodynamic rather than chemostatic behavior of $NO_3 - N$ and *DOC* (Figure 5h), likely due to decreasing streamflow variability with catchment size, in combination with small changes in variability of substances exported from large parts of the catchments, greater groundwater influences and instream processes. Substances such as *SRP* typically originate from point sources or critical source areas (Sharpley et al., 2009) so that their variability might decrease with increasing catchment size, as is the case for streamflow variability, resulting in no relationship between chemodynamic behavior and catchment size.

Below we discuss the diverse behavior of individual solutes. Dilution dominates for *Ca* (*dil*,*cw* and *dil*,*nh* account for more than 85% of the catchments, Figure 4a), as consistent with studies on both long-term and event time scales (e.g., Herndon et al., 2015; Diamond & Cohen, 2018; L. A. Rose et al., 2018). This indicates source limitation of *Ca*, which is likely to be derived from relatively calcium-poor geogenic sources (Macdonald et al., 2017) and could be considered as reference behavior for catchments with only limited anthropogenic inputs (contrasting to *N*, *P* and *C* species). Clockwise hysteresis of *Ca* linked with higher hydrological variability compared to other hysteresis patterns (Figure S6a) relates to fast response in agreement with the conceptual understanding underlying the classification scheme (Figure 1).

Cl shows heterogeneous $c - Q$ response (Figure 4b), whereby dilution with clockwise hysteresis is most prevalent. Dilution can occur in case of instream *Cl* originating from weathering and atmospheric deposition and has been reported from various studies both as an event response (as in our case often in combination with clockwise hysteresis (Butturini et al., 2006; S. Rose, 2003; L. A. Rose et al., 2018),) and also

based on low-resolution data (Diamond & Cohen, 2018). Road salting may be a reason for enrichment in some catchments, but also for clockwise hysteresis with flushing via surface runoff early in events and later dilution with water from upstream which might especially be the case in smaller more urban catchments with higher *Cl* concentrations (Figure S8, compare Figure S3).

SiO_2 is heterogeneous in its $c - Q$ response with enrichment in 60% of the catchments but no dominant hysteresis pattern (Figure 4c). This heterogeneity relates to previous studies elsewhere which reported catchment specific export regimes including enrichment (Anderson et al., 2000), constancy (Diamond & Cohen, 2018), and dilution (Diamond & Cohen, 2018; Herndon et al., 2015; Moatar et al., 2017) and in terms of hysteresis patterns catchment-specific (House & Warwick, 1998) or event-specific response including clockwise (L. A. Rose et al., 2018) and anticlockwise (Scanlon et al., 2001) hysteresis. This can be interpreted as biogenic sources of *Si* (Cornelis et al., 2011; Song et al., 2014), for example, manure, masking the signal expected from the silicate rich geology (Macdonald et al., 2017) thus hindering its use as a conservative tracer for purely hydrologically controlled $c - Q$ behavior.

Despite differences in $c - Q$ classification, *Ca*, *Cl* and SiO_2 agree in predominantly chemostatic behavior (Figures 5a–5c; whereby chemostatic behavior of *Ca* and SiO_2 coincides with high concentrations, Figures S9a and S9c). This is consistent with chemostasis of weathering products often related to hydrologically controlled solute fluxes and large, as well as relatively homogeneous element storage in catchments (Hunsaker & Johnson, 2017; Koger et al., 2018; Musolff et al., 2015; L. A. Rose et al., 2018). Chemodynamic behavior for *Ca* and SiO_2 in some upland catchments (Figures S7a and S7c) can be explained by shorter transit times and is consistent with findings by Musolff et al. (2015) who found chemodynamic behavior in catchments with higher topographic gradient. The association between chemodynamic behavior and high streamflow variability in catchments on the west coast of Scotland may be explained by high rainfall and high atmospheric *Cl* deposition on the Atlantic seaboard.

The heterogeneous $c - Q$ response of $NH_4 - N$ with almost equal representation of export regimes but predominantly chemodynamic behavior (Figures 4d and 5d) may relate to heterogeneous distribution of this solute in the catchment due to point sources, that is, sewage, and high reactivity. These findings are consistent with studies showing differing $c - Q$ patterns of $NH_4 - N$ among catchments (Aguilera & Melack, 2018) and events (L. A. Rose et al., 2018) and predominantly chemodynamic behavior (Musolff et al., 2015; L. A. Rose et al., 2018). Dilution in upland catchments and enrichment in lowland catchments indicates source limited export of $NH_4 - N$ (Figure S7d). In case of constancy, clockwise hysteresis of $NH_4 - N$ is linked to higher hydrological variability indicating faster response (Figure S6d).

Catchment-specific $c - Q$ response of $NO_3 - N$ (Figure 4e) is consistent with other studies (Bowes et al., 2014). Moatar et al. (2017) as well as Ebeling et al. (2021) did not find strong variations between catchments but a dominance of enrichment with more than two thirds of enrichment patterns in French and German studies. Similar to findings on event scales in relatively pristine catchments (Aguilera & Melack, 2018; Butturini et al., 2006; Rusjan et al., 2008; Vaughan et al., 2017), we often observe enrichment with anticlockwise hysteresis. Consistent with Moatar et al. (2017) we found dilution in wet catchments (in our case high runoff and stream-flow variability) indicating high volumes of water available for transport (Figure 6b). We did not find a clear association between $NO_3 - N$ export regime and upland versus lowland catchments possibly related to a combination of point and diffuse sources and surface and subsurface pathways in Scottish catchments with relatively low groundwater $NO_3 - N$ concentrations. Predominantly anticlockwise hysteresis which is further linked with higher hydrological variability can be explained by both sub-surface solute transport leading to later concentration peaks than hydrograph peaks and dilution of downstream urban and agricultural sources with cleaner water from upstream in the relatively large catchments considered in this study. Using the same classification presented in this study, Hashemi et al. (2020) showed predominantly clockwise or no hysteresis likely related to smaller catchment size in their study. Similar to other studies (Dupas et al., 2016; Thompson et al., 2011; Zhong et al., 2017), predominantly chemostatic behavior of $NO_3 - N$ (Figure 5g) may relate to transport limitation especially in catchments with high proportions of intense agriculture. Chemodynamic behavior of $NO_3 - N$ in upland catchments (Figure 6e) and often those with low concentrations (Figure S9e) can be attributed to low anthropogenic impacts and hence source-limitation in agreements with findings elsewhere (e.g., Basu et al., 2010; Diamond & Cohen, 2018; Ebeling et al., 2021).

We found heterogeneous export of *SRP* with predominantly clockwise hysteresis and chemodynamic behavior (Figures 4e and 5e) which have also been reported from other studies on long-term and event scales (Aguilera & Melack, 2018; Hashemi et al., 2020; Moatar et al., 2017). This heterogeneity as well as contrasting associations with catchment characteristics may relate to small or heterogeneous stores of potentially mobilizable sources (Musolff et al., 2015) alongside dilution of point sources and enrichment of diffuse sources (Bowes et al., 2008). Other explanations for heterogeneous export regimes include high reactivity and interactions with other nutrient species and landscape drivers (Glendell et al., 2019; Stutter et al., 2018). A tendency toward dilution and clockwise hysteresis was found in lowland catchments with large proportions of area under artificial drainage and relatively high *SRP* concentrations (Figures S6e and S8f). This may relate to a combination of "first flush" responses (Lee et al., 2002) and dilution with *SRP* poor water from more pristine areas upstream. Clockwise hysteresis generally indicates close proximity or high connectivity between *P* sources and streams to point sources and artificial drainage as short cuts of *P* exports (T. E. Jordan et al., 1997; Koch et al., 2018). A coincidence of anticlockwise hysteresis and enrichment of *SRP* in upland catchment can also be an indication of low influence of point source inputs of *SRP* and geographically distant diffuse sources. Further, a tendency toward clockwise hysteresis of *SRP* in small catchments (anticlockwise hysteresis of *SRP* only in catchments above 200 km^2, Figure 4) is consistent with mostly clockwise hysteresis in small North European catchments (Hashemi et al., 2020) and highlights the importance of understanding *P* mobilization in headwaters (Abbott et al., 2018; Bol et al., 2018; Dupas et al., 2017). Predominantly chemodynamic *SRP* export is consistent with findings for *P* in Germany (Ebeling et al., 2021).

Predominantly enrichment behavior for *DOC* (Figure 4g) agrees with findings on event (Butturini et al., 2006; L. A. Rose et al., 2018) and longer time scales (Herndon et al., 2015; Moatar et al., 2017) related to transport-limited mobilization due to flushing from soils and diffuse carbon sources. The response in Scottish catchments does not show associations with large carbon stocks in organo-mineral and peat soil. As these soils are located in the upper parts of the catchments their signal is masked by sources further downstream in the large and heterogeneous catchments. Enrichment and clockwise hysteresis are linked to high hydrological variability and thus a fast response to individual events (Figure S6f) consistent with the conceptual understanding underlying the classification scheme (Figure 1). A strong variation in hysteresis patterns is consistent with observations for individual events (Butturini et al., 2006) and may be related to the proximity of diffuse sources. Predominantly chemostatic behavior (Figure 5g) is similar to findings in other studies (Dupas et al., 2016; Thompson et al., 2011; Zhong et al., 2017). The definition of chemodynamic behavior by the ratio between coefficients of variation of concentration and discharge may explain chemodynamic behavior of *DOC* in catchments with low streamflow variability (Figure S7f) as small differences in concentration variability between catchments mean that those with lower streamflow variability are considered as chemodynamic and others as chemostatic. The calculation of *CV* for discharge using all discharge data and those of concentrations based on monthly concentration data might additionally influence these results.

4.2. Novel Reproducible Classification of $c - Q$ Relationships of Low-Frequency Data Gives Insights Into Solute Export Behavior in Catchments

By combining information on export regimes (i.e., general relationship between concentration and discharge magnitude) and long-term average hysteresis patterns the proposed classification of $c - Q$ relationships (Figure 1) gives insights into solute export from catchments utilizing long-term low-frequency water quality data. Reproducibility is obtained by evaluating both export regimes and hysteresis patterns based on fitted $c - Q$ models and statistical tests. Previous frameworks categorizing hysteresis patterns (Evans & Davies, 1998; Zuecco et al., 2016) require high-frequency data to analyze individual runoff events. Studies assessing $c - Q$ relationships for low-frequency water quality data typically focus on the slope between concentration and discharge (e.g., Bieroza et al., 2018; Duncan et al., 2017; Hunsaker & Johnson, 2017). A classification developed by Moatar et al. (2017) considers $c - Q$ dynamics of low-frequency data more explicitly by fitting separate $c - Q$ relationships for high and low flows. The classification proposed in our study follows on from Moatar et al. (2017) and additionally considers hysteresis patterns in low-frequency data by comparing rising and falling hydrograph limbs.

The proposed classification allows for a rapid and reproducible assessment of average long-term $c - Q$ relationships. Solute-specific and spatially heterogeneous patterns which can be related to contrasting catchment characteristics in terms of climate, topography, land cover and soil indicate the applicability of the method to group catchments according to their $c - Q$ response using widely available low-resolution water quality data. We appreciate that investigating high-resolution data can result in seasonally different (Bieroza & Heathwaite, 2015; Duncan et al., 2017; Minaudo et al., 2019) and event specific $c - Q$ relationships (Aguilera & Melack, 2018; Knapp et al., 2020). These dynamics are mostly not considered when assessing $c - Q$ relationships based on long-term low-frequency data, so that especially constancy and no hysteresis might reflect contrasting dynamics at different temporal scales. Other studies, however, report relatively stable $c - Q$ responses among events (L. A. Rose et al., 2018). As highlighted in other studies (Dupas et al., 2016; L. A. Rose et al., 2018), combining long-term low-resolution and short-term high-resolution data is promising to get insights into controlling factors of solute exports in the absence of long-term high-resolution data. For that, the classification presented here could be used to compare event responses based on high-frequency data with average long-term $c - Q$ relationships. To investigate the effect of data resolution, the classification can further be applied to high-resolution data and to low-resolution data sub-sampled from these high-resolution data. It would further be interesting to analyze to what extent assessing chemostatic versus chemodynamic behavior is affected by the temporal resolution of concentration data. In case of low-resolution concentration data, comparing CV based on all discharge data with CV of discharge considering only dates when concentration data are available might be of interest.

The power-law $c - Q$ models (Equation 2) underlying the classification are flexible and allow to consider different behavior for low and high discharge and hysteresis patterns also allowing for a better estimation of concentrations from discharge shown in Figure S5 in terms of Pearson correlations between observed and modeled concentrations. These $c - Q$ models are applicable beyond the purpose of classification, for example, for more robust load estimation which generally improves when $c - Q$ dynamics are taken into account (Diamond & Cohen, 2018). However, applying these complex models might pose the risk of overparametrization. The proposed $c - Q$ classification shown in Figure 1 is versatile and applicable to other $c - Q$ models that consider concentration changes with discharge and hysteresis patterns. The classification presented here could be extended to consider more complex patterns, such as changing $c - Q$ slopes, for example, dilution at low flows and enrichment at high flows which have been reported from various studies (e.g., Bowes et al., 2014; Hunsaker & Johnson, 2017). In our classification, these patterns are summarized as constancy, but it could be interesting to distinguish more types of $c - Q$ by investigating more complex patterns. To that end, the $c - Q$ models presented here (Equation 2) with different equations for discharge below and above an automatically derived threshold could be utilized. In order to form a basis for a classification of more complex export regimes it might be necessary to modify the approach to determine streamflow thresholds for segmented $c - Q$ models for example, by constraining the optimization algorithm to ranges of discharge quantiles to be considered as high flow and low flow instead of allowing for segmentation at any discharge quantile. By giving insights into temporal patterns of solute exports the proposed classification could support temporal targeting of mitigation measures, a strategy suggested by Preisendanz et al. (2021).

Although discharge and concentration are integrated both in the $c - Q$ classification and in the analysis of chemodynamic versus chemostatic behavior and also $c - Q$ slopes and the ratio of coefficients of variation between concentration and discharge are mathematically not independent (Jawitz & Mitchell, 2011), there are no obvious overlaps between these categorizations (compare Figures 4 and 5, see Figure S10). Musolff et al. (2015) also described chemodynamic versus chemostatic behavior and patterns between concentration and discharge magnitude as separate categories, the latter expressed by the slope of the power-law $c - Q$ model. In that sense, (a) export regime, (b) hysteresis and (c) chemodynamic versus chemostatic behavior could be combined in a reproducible three-dimensional classification. Such a classification would relate to the categorization by Evans and Davies (1998) who considered patterns between concentration and discharge magnitude (i.e., export regime), hysteresis, and curvature (comparing discharge and concentration variability analogical to chemodynamic vs. chemostatic behavior) for describing individual runoff events based on high-frequency data but would be novel in its applicability to low-frequency water quality data and hence potentially more widely applicable to more catchments where low resolution monitoring data is available.

4.3. Combining $c - Q$ Behavior and Information on Catchment Characteristics Can Be Used for Grouping Catchments

The classification of $c - Q$ relationships is associated with catchment characteristics, mainly with respect to upland versus lowland catchments and streamflow variability (Figure 6). This confirms our hypothesis that $c - Q$ classification of long-term low-frequency data can identify and group solute export behaviors. However, in line with other studies (Butturini et al., 2006; Diamond & Cohen, 2018; Godsey et al., 2009; Musolff et al., 2015), we have not been able to identify dominant influences on the individual solute exports. Multiple confounding factors in the relatively large and heterogeneous catchments (Figure 3) are likely to affect the links between catchment characteristics and $c - Q$ relationships (Ali et al., 2017; Glendell et al., 2019; Musolff et al., 2015). These include seasonality effects on $c - Q$ relationships (Minaudo et al., 2019) and point sources weakening the influence of land cover proportions in the entire catchment (Zhou et al., 2017). For example, down-stream point sources might be the reason why *DOC* export is not predominantly associated with histosols as upstream carbon source. In addition, while the *MFA* allows to relate solute responses to catchment characteristics overall, it does not allow determining the impact of individual catchment characteristics on solute responses within individual catchments, primarily due to the relatively small number of catchments included and correlations between catchment characteristics.

Comparing patterns in nested catchments, similar to Müller et al. (2018) and Kändler et al. (2017), would allow taking landscape characteristics into account that influence solute mobilization and retention. Investigating soil spatial heterogeneity (Glendell et al., 2014) could be promising as similar proportions of soils but in different locations may result in different influences on water quality at monitoring sites, whereby some responses to dominant soil-hydrological flow pathways may be masked by downstream influences. Investigating a greater number of catchments in a single comparative study could allow greater statistical power and hence identify landscape controls on $c - Q$ relationships and chemodynamic versus chemostatic behavior with greater certainty.

As solute behavior vary both between solutes and catchments and are related to catchment characteristics, we recommend future catchment typologies aimed at water quality should consider both physical catchment characteristics and solute response rather than being derived from catchment characteristics alone, as is currently the case with several water framework directive classifications. The importance of streamflow variability for solute exports (Deelstra & Iital, 2008; P. Jordan et al., 2005), shown by the association between streamflow indices and $c - Q$ types and chemodynamic versus chemostatic behavior (Figures 6a and 6d) in our study indicates that catchment typologies should also consider streamflow response.

5. Conclusion and Outlook

We developed a novel reproducible classification of $c - Q$ relationships integrating export regime (enrichment, constancy, dilution) and long-term average hysteresis patterns (clockwise, no hysteresis, and anticlockwise) applicable to low-frequency water quality data. The proposed $c - Q$ classification allows maximizing the information content of long-term low-frequency water quality data typical for regulatory monitoring.

The classification was applied to 45 Scottish catchments representing contrasting landscape conditions. We found that the $c - Q$ types are both solute- and catchment specific which also shows that $c - Q$ classification of long-term low-frequency data can identify and group solute export behaviors. Export regimes of Cl, SiO_2, $NH_4 - N$, $NO_3 - N$ and SRP differ strongly between catchments whereas Ca shows mostly dilution and DOC enrichment or constancy. Clockwise hysteresis prevails for $NH_4 - N$ and SRP, anticlockwise hysteresis for $NO_3 - N$ with stronger variation for the other solutes. Chemodynamic versus chemostatic behavior which was additionally assessed is generally solute specific with predominantly chemodynamic response of $NH_4 - N$ and SRP and chemostatic response of Ca, Cl, SiO_2, $NO_3 - N$ and DOC.

Upland versus lowland catchment characteristics as well as streamflow variability have been identified as the main influences on $c - Q$ classification and chemodynamic versus chemostatic behavior. Despite links between catchment characteristics and $c - Q$ classification as well as chemodynamic versus chemostatic behavior, dominant catchment controls for all solutes could not be identified. Further, $c - Q$ relationships

are not associated with chemodynamic versus chemostatic behavior. This indicates that future catchment typologies should combine a response-led analysis, that is, $c - Q$ relationships, chemodynamic versus chemostatic behavior as well as streamflow variability, with information on physical characteristics such as hydroclimatic conditions, topography, land cover, and soil to inform pollution mitigation measures and cost-effective monitoring design.

Future applications of the reproducible $c - Q$ classification developed in this study to a larger number of catchments in contrasting landscapes as well as nested catchments may help to identify catchment controls on solute exports. Utilizing the classification to compare low and high-frequency data could help to understand the extent of information loss. As solute exports from catchments respond to changing environmental conditions and extreme hydroclimatic events, analyzing temporal changes in $c - Q$ classification, discharge and concentration variability could help to identify dominant controls on solute exports, assess potential impacts of future environmental change and evaluate the effectiveness of pollution mitigation measures.

Data Availability Statement

The data used in this study were provided by the Scottish Environment Protection Agency and are used as part of their environmental monitoring and regulatory reporting. The Terms and Conditions of Use of Data under which they were supplied for this research specifies they cannot be shared with any Third party. Instead, data can be requested directly from DataRequests@sepa.org.uk. Air temperature and precipitation data have been obtained from the UK Met Office, land cover has been derived from the Land Cover Map 2007 (LCM2007) by the Centre for Ecology and Hydrology. Soils data have been obtained from the National soil map of Scotland (1:250,000) "Soil Survey of Scotland Staff (1981). Macaulay Institute for Soil Research, Aberdeen." https://www.hutton.ac.uk/learning/natural-resource-datasets/soils/quarter-million-soils.

Acknowledgments
The project was funded by the Rural and Environment Science and Analytical Services (RESAS) Division of the Scottish Government. Javier Palarea-Albaladejo was partly supported by the Spanish Ministry of Science, Innovation and Universities (CODAMET RTI2018-095518-B-C21, 2019–2021). We would like to acknowledge Allan Lilly and Mads Troldborg (James Hutton Institute) for helpful comments on an earlier version of the manuscript. We are grateful to four anonymous reviewers and the associate editor Jean Bahr for their valuable comments and constructive suggestions which helped to improve the manuscript significantly. Michèl Pohle is acknowledged for proofreading and LaTeX technical support.

References

Abbott, B. W., Gruau, G., Zarnetske, J. P., Moatar, F., Barbe, L., Thomas, Z., et al. (2018). Unexpected spatial stability of water chemistry in headwater stream networks. *Ecology Letters*, *21*(2), 296–308. https://doi.org/10.1111/ele.12897

Abdi, H., Williams, L. J., & Valentin, D. (2013). Multiple factor analysis: Principal component analysis for multitable and multiblock data sets. *Wiley Interdisciplinary Reviews: Computational Statistics*, *5*(2), 149–179. https://doi.org/10.1002/wics.1246

Aguilera, R., & Melack, J. M. (2018). Concentration-discharge responses to storm events in coastal california watersheds. *Water Resources Research*, *54*(1), 407–424. https://doi.org/10.1002/2017WR021578

Ali, G., Wilson, H., Elliott, J., Penner, A., Haque, A., Ross, C., & Rabie, M. (2017). Phosphorus export dynamics and hydrobiogeochemical controls across gradients of scale, topography and human impact. *Hydrological Processes*, *31*(18), 3130–3145. https://doi.org/10.1002/hyp.11258

Anderson, S. P., Drever, J. I., Frost, C. D., & Holden, P. (2000). Chemical weathering in the foreland of a retreating glacier. *Geochimica et Cosmochimica Acta*, *64*(7), 1173–1189. Retrieved from http://www.sciencedirect.com.libezproxy.open.ac.uk/science/article/pii/S0016703799003580

Arheimer, B., & Lidén, R. (2000). Nitrogen and phosphorus concentrations from agricultural catchments - Influence of spatial and temporal variables. *Journal of Hydrology*, *227*(1–4), 140–159. https://doi.org/10.1016/S0022-1694(99)00177-8

Baggaley, N., Poggio, L., Gimona, A., & Lilly, A. (2016). Comparison of traditional and geostatistical methods to estimate and map the carbon content of Scottish soils. In G. Zhang, D. Brus, F. Liu, X. Song, & P. Lagacherie (Eds.), *Digital soil mapping across paradigms, scales and boundaries* (pp. 103–111). Springer Singapore. https://doi.org/10.1007/978-981-10-0415-5_9

Baker, D. B., Richards, R. P., Loftus, T. T., & Kramer, J. W. (2004). A new flashiness index: Characteristics and applications to Midwestern rivers and streams. *Journal of the American Water Resources Association*, *40*(2), 503–522. https://doi.org/10.1111/j.1752-1688.2004.tb01046.x

Basu, N. B., Destouni, G., Jawitz, J. W., Thompson, S. E., Loukinova, N. V., Darracq, A., et al. (2010). Nutrient loads exported from managed catchments reveal emergent biogeochemical stationarity. *Geophysical Research Letters*, *37*(23), 1–n. https://doi.org/10.1029/2010GL045168

Basu, N. B., Thompson, S. E., & Rao, P. S. C. (2011). Hydrologic and biogeochemical functioning of intensively managed catchments: A synthesis of top-down analyses. *Water Resources Research*, *47*(10), 1–12. https://doi.org/10.1029/2011WR010800

Bieroza, M. Z., & Heathwaite, A. L. (2015). Seasonal variation in phosphorus concentration-discharge hysteresis inferred from high-frequency in situ monitoring. *Journal of Hydrology*, *524*, 333–347. https://doi.org/10.1016/j.jhydrol.2015.02.036

Bieroza, M. Z., Heathwaite, A. L., Bechmann, M., Kyllmar, K., & Jordan, P. (2018). The concentration-discharge slope as a tool for water quality management. The *Science of the Total Environment*, *630*, 738–749. https://doi.org/10.1016/j.scitotenv.2018.02.256

Bol, R., Gruau, G., Mellander, P.-E., Dupas, R., Bechmann, M., Skarbøvik, E., et al. (2018). Challenges of reducing phosphorus based water eutrophication in the agricultural landscapes of northwest Europe. *Frontiers in Marine Science*, *5*(August), 1–16. https://doi.org/10.3389/fmars.2018.00276

Bond, N. (2016). hydrostats. Hydrologic indices for daily time series data. R package. R-Package.

Boorman, D. B., Hollis, J. M., & Lilly, A. (1995). *Hydrology of soil types: A Hydrologically-Based classification of the soils of United Kingdom* (Vol. 137). Institute of Hydrology. Retrieved from http://nora.nerc.ac.uk/7369/

Bowes, M. J., Jarvie, H. P., Naden, P. S., Old, G. H., Scarlett, P. M., Roberts, C., et al. (2014). Identifying priorities for nutrient mitigation using river concentration-flow relationships: The Thames basin, UK. *Journal of Hydrology*, *517*, 1–12. https://doi.org/10.1016/j.jhydrol.2014.03.063

Bowes, M. J., Smith, J. T., Jarvie, H. P., & Neal, C. (2008). Modelling of phosphorus inputs to rivers from diffuse and point sources. *The Science of the Total Environment*, *395*(2–3), 125–138. https://doi.org/10.1016/j.scitotenv.2008.01.054

Bracken, L., Wainwright, J., Ali, G., Tetzlaff, D., Smith, M., Reaney, S., & Roy, A. (2013). Concepts of hydrological connectivity: Research approaches, pathways and future agendas. *Earth-Science Reviews*, *119*, 17–34. https://doi.org/10.1016/j.earscirev.2013.02.001

Butturini, A., Gallart, F., Latron, J., Vazquez, E., & Sabater, F. (2006). Cross-site comparison of variability of DOC and nitrate c-q hysteresis during the autumn-winter period in three Mediterranean headwater streams: A synthetic approach. *Biogeochemistry*, *77*(3), 327–349. https://doi.org/10.1007/s10533-005-0711-7

Causse, J., Baurès, E., Mery, Y., Jung, A.-V., & Thomas, O. (2015). Variability of N export in water: A review. *Critical Reviews in Environmental Science and Technology*, *45*, 2245–2281. https://doi.org/10.1080/10643389.2015.1010432

Chapman, S. J., Bell, J., Donnelly, D., & Lilly, A. (2009). Carbon stocks in Scottish peatlands. *Soil Use and Management*, *25*(2), 105–112. https://doi.org/10.1111/j.1475-2743.2009.00219.x

Cornelis, J. T., Delvaux, B., Georg, R. B., Lucas, Y., Ranger, J., & Opfergelt, S. (2011). Tracing the origin of dissolved silicon transferred from various soil-plant systems towards rivers: A review. *Biogeosciences*, *8*(1), 89–112. https://doi.org/10.5194/bg-8-89-2011

Creed, I. F., & Band, L. E. (1998). Export of nitrogen from catchments within a temperate forest: Evidence for a unifying mechanism regulated by variable source area dynamics. *Water Resources Research*, *34*(11), 3105–3120. https://doi.org/10.1029/98WR01924

Creed, I. F., Mcknight, D. D. M., Pellerin, B. A., Green, M. B., Bergamaschi, B. A., Aiken, G. R., et al. (2015). The river as a chemostat: Fresh perspectives on dissolved organic matter flowing down the river continuum. *Canadian Journal of Fisheries and Aquatic Sciences*, *14*(April), 1–1285. https://doi.org/10.1139/cjfas-2014-0400

Deelstra, J., & Iital, A. (2008). The use of the flashiness index as a possible indicator for nutrient loss prediction in agricultural catchments. *Boreal Environment Research*, *13*(3), 209–221.

Deelstra, J., Iital, A., Povilaitis, A., Kyllmar, K., Greipsland, I., Blicher-Mathiesen, G., et al. (2014). Reprint of "Hydrological pathways and nitrogen runoff in agricultural dominated catchments in Nordic and Baltic countries". *Agriculture, Ecosystems and Environment*, *198*, 65–219. https://doi.org/10.1016/j.agee.2014.06.007

Diamond, J. S., & Cohen, M. J. (2018). Complex patterns of catchment solute–discharge relationships for coastal plain rivers. *Hydrological Processes*, *32*(3), 388–401. https://doi.org/10.1002/hyp.11424

Duncan, J. M., Band, L. E., & Groffman, P. M. (2017). Variable nitrate concentration–discharge relationships in a forested watershed. *Hydrological Processes*, *31*(9), 1817–1824. https://doi.org/10.1002/hyp.11136

Duncan, J. M., Band, L. E., Groffman, P. M., & Bernhardt, E. S. (2015). Mechanisms driving the seasonality of catchment scale nitrate export: Evidence for riparian ecohydrologic controls. *Water Resources Research*, *51*(6), 3982–3997. https://doi.org/10.1002/2015WR016937

Dupas, R., Jomaa, S., Musolff, A., Borchardt, D., & Rode, M. (2016). Disentangling the influence of hydroclimatic patterns and agricultural management on river nitrate dynamics from sub-hourly to decadal time scales. *The Science of the Total Environment*, *571*, 791–800. https://doi.org/10.1016/j.scitotenv.2016.07.053

Dupas, R., Musolff, A., Jawitz, J. W., Rao, P. S. C., Jäger, C. G., Fleckenstein, J. H., et al. (2017). Carbon and nutrient export regimes from headwater catchments to downstream reaches. *Biogeosciences*, *14*(18), 4391–4407. https://doi.org/10.5194/bg-14-4391-2017

Ebeling, P., Kumar, R., Weber, M., Knoll, L., Fleckenstein, J. H., & Musolff, A. (2021). Archetypes and controls of riverine nutrient export across German catchments. *Water Resouces Research*, *57*(4), 1–29. https://doi.org/10.1029/2020wr028134

Elzhov, T. V., Mullen, K. M., Spiess, A.-N., & Bolker, B. (2016). *Minpack.lm. R interface to the Levenberg-Marquardt nonlinear least-squares algorithm found in MINPACK, plus support for bounds. R package*.

Evans, C., & Davies, T. D. (1998). Causes of concentration/discharge hysteresis and its potential as a tool for analysis of episode hydrochemistry. *Water Resources Research*, *34*(1), 129–137. https://doi.org/10.1029/97WR01881

Fischer, P., Pöthig, R., & Venohr, M. (2017). The degree of phosphorus saturation of agricultural soils in Germany: Current and future risk of diffuse P loss and implications for soil P management in Europe. *The Science of the Total Environment*, *599–600*, 1130–1139. https://doi.org/10.1016/j.scitotenv.2017.03.143

Glendell, M., Granger, S. J., Bol, R., & Brazier, R. E. (2014). Quantifying the spatial variability of soil physical and chemical properties in relation to mitigation of diffuse water pollution. *Geoderma*, *214–215*, 25–41. https://doi.org/10.1016/j.geoderma.2013.10.008

Glendell, M., Palarea-Albaladejo, J., Pohle, I., Marrero, S., McCreadie, B., Cameron, G., & Stutter, M. (2019). Modeling the ecological impact of phosphorus in catchments with multiple environmental stressors. *Journal of Environmental Quality*, *48*(5), 1336–1346. https://doi.org/10.2134/jeq2019.05.0195

Godsey, S. E., Kirchner, J. W., & Clow, D. W. (2009). Concentration–discharge relationships reflect chemostatic characteristics of US catchments. *Hydrological Processes*, *23*, 1844–1864. https://doi.org/10.1002/hyp10.1002/hyp.7315

Guillemot, S., Fovet, O., Gascuel-Odoux, C., Gruau, G., Casquin, A., Curie, F., & Moatar, F. (2020). Spatio-temporal controls of C-N-P dynamics across headwater catchments of a temperate agricultural region from public data analysis. *Hydrology and Earth System Sciences*, *25*(3), pp. 1–31. https://doi.org/10.5194/hess-2020-257?utm10.5194/hess-2020-257

Guo, D., Lintern, A., Webb, J. A., Ryu, D., Liu, S., Bende-Michl, U., et al. (2019). Key factors affecting temporal variability in stream water quality. *Water Resources Research*, *55*(1), 112–129. https://doi.org/10.1029/2018WR023370

Hadley Centre for Climate Prediction and Research. (2017). *UKCP09: Land and marine past climate and future scenario projections data for the UK*. Centre for Environmental Data Analysis. Retrieved from http://catalogue.ceda.ac.uk/uuid/094d9c9b9dda42c0aa1a1848af9fb56b

Hashemi, F., Pohle, I., Pullens, J., Tornbjerg, H., Kyllmar, K., Marttila, H., & Kronvang, B. (2020). Conceptual mini-catchment typologies for testing dominant controls of nutrient dynamics in three Nordic countries. *Water*, *12*(1776), 1–17. https://doi.org/10.3390/w12061776

Heathwaite, A. L., Quinn, P. F., & Hewett, C. J. (2005). Modelling and managing critical source areas of diffuse pollution from agricultural land using flow connectivity simulation. *Journal of Hydrology*, *304*(1–4), 446–461. https://doi.org/10.1016/j.jhydrol.2004.07.043

Herndon, E. M., Dere, A. L., Sullivan, P. L., Norris, D., Reynolds, B., & Brantley, S. L. (2015). Landscape heterogeneity drives contrasting concentration-discharge relationships in shale headwater catchments. *Hydrology and Earth System Sciences*, *19*(8), 3333–3347. https://doi.org/10.5194/hess-19-3333-2015

Hewett, C. J. M., Quinn, P. F., Whitehead, P. G., Heathwaite, A. L., & Flynn, N. J. (2004). Towards a nutrient export risk matrix approach to managing agricultural pollution at source. *Hydrological and Earth System Sciences*, *8*(4), 834–845. https://doi.org/10.5194/hess-8-834-2004

House, W. A., & Warwick, M. S. (1998). Hysteresis of the solute concentration/discharge relationship in rivers during storms. *Water Research*, *32*(8), 2279–2290. https://doi.org/10.1016/S0043-1354(97)00473-9

Hunsaker, C. T., & Johnson, D. W. (2017). Concentration-discharge relationships in headwater streams of the Sierra Nevada, California. *Water Resources Research*, *53*(9), 7869–7884. https://doi.org/10.1002/2016WR019693

Jawitz, J. W., & Mitchell, J. (2011). Temporal inequality in catchment discharge and solute export. *Water Resources Research*, *47*(10), 1–16. https://doi.org/10.1029/2010wr010197

Jordan, P., Menary, W., Daly, K., Kiely, G., Morgan, G., Byrne, P., & Moles, R. (2005). Patterns and processes of phosphorus transfer from Irish grassland soils to rivers - Integration of laboratory and catchment studies. *Journal of Hydrology*, *304*(1–4), 20–34. https://doi.org/10.1016/j.jhydrol.2004.07.021

Jordan, T. E., Correll, D. L., & Weller, D. E. (1997). Relating nutrient discharges from watersheds. *Water Resources Research*, *33*(11), 2579–2590. https://doi.org/10.1029/97wr02005

Kändler, M., Blechinger, K., Seidler, C., Pavlâu, V., Šanda, M., Dostál, T., et al. (2017). Impact of land use on water quality in the upper Nisa catchment in the Czech Republic and in Germany. The *Science of the Total Environment*, *586*, 1316–1325. https://doi.org/10.1016/j.scitotenv.2016.10.221

Knapp, J. L. A., von Freyberg, J., Studer, B., Kiewiet, L., & Kirchner, J. W. (2020). Concentration-discharge relationships vary among hydrological events, reflecting differences in event characteristics. *Hydrology and Earth System Sciences*, *24*(5), 2561–2576. https://doi.org/10.5194/hess-24-2561-2020

Koch, S., Kahle, P., & Lennartz, B. (2018). Spatio-temporal analysis of phosphorus concentrations in a North-Eastern German lowland watershed. *Journal of Hydrology: Regional Studies*, *15*(February), 203–216. https://doi.org/10.1016/j.ejrh.2018.02.001

Koger, J. M., Newman, B. D., & Goering, T. J. (2018). Chemostatic behaviour of major ions and contaminants in a semiarid spring and stream system near Los Alamos, NM, USA. *Hydrological Processes*, *32*(11), 1709–1716. https://doi.org/10.1002/hyp.11624

Krause, S., Freer, J., Hannah, D. M., Howden, N. J. K., Wagener, T., & Worrall, F. (2014). Catchment similarity concepts for understanding dynamic biogeochemical behaviour of river basins. *Hydrological Processes*, *28*(3), 1554–1560. https://doi.org/10.1002/hyp.10093

Lawler, D. M., Petts, G. E., Foster, I. D., & Harper, S. (2006). Turbidity dynamics during spring storm events in an urban headwater river system: The Upper Tame, West Midlands, UK. *The Science of the Total Environment*, *360*(1–3), 109–126. https://doi.org/10.1016/j.scitotenv.2005.08.032

Le, S., Josse, J., & Husson, F. (2008). FactoMineR: An R package for multivariate analysis. *Journal of Statistical Software*, *25*(1), 1–18. https://doi.org/10.18637/jss.v025.i01

Lee, J., Bang, K., Kethurn, L., Choe, J., & Yu, M. J. (2002). First flush analysis of urban storm rain. The *Science of the Total Environment*, *293*, 163–175. https://doi.org/10.1016/S0048-9697(02)00006-2

Lepistö, A., Granlund, K., Kortelainen, P., & Räike, A. (2006). Nitrogen in river basins: Sources, retention in the surface waters and peatlands, and fluxes to estuaries in Finland. *The Science of the Total Environment*, *365*(1–3), 238–259. https://doi.org/10.1016/j.scitotenv.2006.02.053

Li, L., Bao, C., Sullivan, P. L., Brantley, S., Shi, Y., & Duffy, C. (2017). Understanding watershed hydrogeochemistry: 2. Synchronized hydrological and geochemical processes drive stream chemostatic behavior. *Water Resources Research*, *53*(3), 2346–2367. https://doi.org/10.1002/2016WR018935

Lilly, A., Baggaley, N., Rees, B., Topp, K., Dickson, I., & Elrick, G. (2012). *Report on agricultural drainage and greenhouse gas abatement in Scotland (Tech. Rep.). Prepared on behalf of ClimateXChange*. James Hutton Institute and Scottish Rural College.

Lintern, A., Webb, J. A., Ryu, D., Liu, S., Waters, D., Leahy, P., et al. (2018). What are the key catchment characteristics affecting spatial differences in riverine water quality? *Water Resources Research*, *54*(10), 7252–7272. https://doi.org/10.1029/2017WR022172

Macdonald, A., Dochartaigh, B., & Smedley, P. (2017). *Baseline groundwater chemistry in Scotland's aquifers*. British Geological Survey Open. Reports OR/17/30.

Mellander, P. E., Jordan, P., Shore, M., Melland, A. R., & Shortle, G. (2015). Flow paths and phosphorus transfer pathways in two agricultural streams with contrasting flow controls. *Hydrological Processes*, *29*(16), 3504–3518. https://doi.org/10.1002/hyp.10415

Meybeck, M., & Moatar, F. (2012). Daily variability of river concentrations and fluxes: Indicators based on the segmentation of the rating curve. *Hydrological Processes*, *26*(8), 1188–1207. https://doi.org/10.1002/hyp.8211

Miller, M. P., Tesoriero, A. J., Hood, K., Terziotti, S., & Wolock, D. M. (2017). Estimating discharge and nonpoint source nitrate loading to streams from three end-member pathways using high-frequency water quality data. *Water Resources Research*, *53*(12), 10201–10216. https://doi.org/10.1002/2017WR021654

Minaudo, C., Dupas, R., Gascuel-Odoux, C., Roubeix, V., Danis, P.-A., & Moatar, F. (2019). Seasonal and event-based concentration-discharge relationships to identify catchment controls on nutrient export regimes. *Advances in Water Resources*, *131*(July), 103379. https://doi.org/10.1016/j.advwatres.2019.103379

Moatar, F., Abbott, B. W., Minaudo, C., Curie, F., & Pinay, G. (2017). Elemental properties, hydrology, and biology interact to shape concentration-discharge curves for carbon, nutrients, sediment, and major ions. *Water Resources Research*, *53*(2), 1270–1287. https://doi.org/10.1002/2016WR019635

Morton, D., Rowland, C., Wood, C., Meek, L., Marston, C., Smith, G., & Simpson, I. (2011). *Final Report for LCM2007 - the new UK land cover map (Tech. Rep.)*. Countryside Survey Technical Report No 11/07 NERC/Centre for Ecology & Hydrology.

Müller, C., Musolff, A., Strachauer, U., Brauns, M., Tarasova, L., Merz, R., & Knöller, K. (2018). Tomography of anthropogenic nitrate contribution along a mesoscale river. *The Science of the Total Environment*, *615*, 773–783. https://doi.org/10.1016/j.scitotenv.2017.09.297

Musolff, A., Fleckenstein, J. H., Opitz, M., Büttner, O., Kumar, R., & Tittel, J. (2018). Spatio-temporal controls of dissolved organic carbon stream water concentrations. *Journal of Hydrology*, *566*(August), 205–215. https://doi.org/10.1016/j.jhydrol.2018.09.011 Retrieved from https://linkinghub.elsevier.com/retrieve/pii/S0022169418306978

Musolff, A., Fleckenstein, J. H., Rao, P. S., & Jawitz, J. W. (2017). Emergent archetype patterns of coupled hydrologic and biogeochemical responses in catchments. *Geophysical Research Letters*, *44*(9), 4143–4151. https://doi.org/10.1002/2017GL072630

Musolff, A., Schmidt, C., Selle, B., & Fleckenstein, J. H. (2015). Catchment controls on solute export. *Advances in Water Resources*, *86*, 133–146. https://doi.org/10.1016/j.advwatres.2015.09.026

Palarea-Albaladejo, J., & Martín-Fernández, J. A. (2015). ZCompositions - R package for multivariate imputation of left-censored data under a compositional approach. *Chemometrics and Intelligent Laboratory Systems*, *143*, 85–96. https://doi.org/10.1016/j.chemolab.2015.02.019

Pawlowsky-Glahn, V., & Buccianti, A. (2011). *Compositional data analysis: Theory and applications*. https://doi.org/10.1002/9781119976462

Preisendanz, H., Veith, T., Zhang, Q., & Shortle, J. (2021). Temporal inequality of nutrient and sediment transport: A decisionmaking framework for temporal targeting of load reduction goals. *Environmental Research Letters*, *16*(014005), 1–17. https://doi.org/10.1088/1748-9326/abc997

Reddy, K. R., Kadlec, R. H., Flaig, E., & Gale, P. M. (1999). Phosphorus retention in streams and wetlands: A review. *Critical Reviews in Environmental Science and Technology*, *29*(1), 83–146. https://doi.org/10.1080/10643389991259182

Richards, S., Paterson, E., Withers, P. J., & Stutter, M. (2016). Septic tank discharges as multi-pollutant hotspots in catchments. *The Science of the Total Environment*, *542*, 854–863. https://doi.org/10.1016/j.scitotenv.2015.10.160

Robert, P., & Escoufier, Y. (1976). A unifying tool for linear multivariate statistical methods: The RV- coefficient. *Applied Statistics*, *25*(3), 257. https://doi.org/10.2307/2347233

Rose, L. A., Karwan, D. L., & Godsey, S. E. (2018). Concentration–discharge relationships describe solute and sediment mobilization, reaction, and transport at event and longer timescales. *Hydrological Processes*, *32*(18), 2829–2844. https://doi.org/10.1002/hyp.13235

Rose, S. (2003). Comparative solute-discharge hysteresis analysis for an urbanized and a 'control basin' in the Georgia (USA) Piedmont. *Journal of Hydrology*, *284*(1–4), 45–56. https://doi.org/10.1016/j.jhydrol.2003.07.001

Rosenberg, B. D., & Schroth, A. W. (2017). Coupling of reactive riverine phosphorus and iron species during hot transport moments: Impacts of land cover and seasonality. *Biogeochemistry*, *132*(1–2), 103–122. https://doi.org/10.1007/s10533-016-0290-9

Rusjan, S., Brilly, M., & Mikoš, M. (2008). Flushing of nitrate from a forested watershed: An insight into hydrological nitrate mobilization mechanisms through seasonal high-frequency stream nitrate dynamics. *Journal of Hydrology*, *354*(1–4), 187–202. https://doi.org/10.1016/j.jhydrol.2008.03.009

Sawicz, K., Wagener, T., Sivapalan, M., Troch, P. A., & Carrillo, G. (2011). Catchment classification: Empirical analysis of hydrologic similarity based on catchment function in the eastern USA. *Hydrology and Earth System Sciences*, *15*(9), 2895–2911. https://doi.org/10.5194/hess-15-2895-2011

Scanlon, T. M., Raffensperger, J. P., & Hornberger, G. M. (2001). Modeling transport of dissolved silica in a forested headwater catchment: Implications for defining the hydrochemical response of observed flow pathways. *Water Resources Research*, *37*(4), 1071–1082. https://doi.org/10.1029/2000WR900278

Sharpley, A. N., Kleinman, P. J., Jordan, P., Bergström, L., & Allen, A. L. (2009). Evaluating the Success of Phosphorus Management from Field to Watershed. *Journal of Environmental Quality*, *38*(5), 1981–1988. https://doi.org/10.2134/jeq2008.0056

Sliva, L., & Williams, D. D. (2001). Buffer zone versus whole catchment approaches to studying land use impact on river water quality. *Water Research*, *35*(November), 3462–3472. https://doi.org/10.1016/S0043-1354(01)00062-8

Soil Survey of Scotland Staff. (1984). *Organisation and methods of the 1:250 000 soil survey of Scotland. Handbook 8 (Tech. Rep.). Aberdeen*. The Macaulay Institute for Soil Research. Retrieved from https://soils.environment.gov.scot/maps/soil-maps/national-soil-map-of-scotland/

Song, Z., Wang, H., Strong, P. J., & Shan, S. (2014). Increase of available soil silicon by Si-rich manure for sustainable rice production. *Agronomy for Sustainable Development*, *34*(4), 813–819. https://doi.org/10.1007/s13593-013-0202-5

Stutter, M. I., Graeber, D., Evans, C. D., Wade, A. J., & Withers, P. J. (2018). Balancing macronutrient stoichiometry to alleviate eutrophication. *The Science of the Total Environment*, *634*, 439–447. https://doi.org/10.1016/j.scitotenv.2018.03.298

Thompson, S. E., Basu, N. B., Lascurain, J., Aubeneau, A., & Rao, P. S. (2011). Relative dominance of hydrologic versus biogeochemical factors on solute export across impact gradients. *Water Resources Research*, *47*(7), 1–20. https://doi.org/10.1029/2010WR009605

Vaughan, M. C., Bowden, W. B., Shanley, J. B., Vermilyea, A., Sleeper, R., Gold, A. J., et al. (2017). High-frequency dissolved organic carbon and nitrate measurements reveal differences in storm hysteresis and loading in relation to land cover and seasonality. *Water Resources Research*, *53*(7), 5345–5363. https://doi.org/10.1002/2017WR020491

Viglione, A., Parajka, J., Rogger, M., Salinas, J. L., Laaha, G., Sivapalan, M., & Blöschl, G. (2013). Comparative assessment of predictions in ungauged basins - Part 3: Runoff signatures in Austria. *Hydrology and Earth System Sciences*, *17*(6), 2263–2279. https://doi.org/10.5194/hess-17-2263-2013

Winnick, M. J., Carroll, R. W., Williams, K. H., Maxwell, R. M., Dong, W., & Maher, K. (2017). Snowmelt controls on concentration-discharge relationships and the balance of oxidative and acid-base weathering fluxes in an alpine catchment, East River, Colorado. *Water Resources Research*, *53*(3), 2507–2523. https://doi.org/10.1002/2016WR019724

Zhong, J., Li, S. L., Tao, F., Yue, F., & Liu, C. Q. (2017). Sensitivity of chemical weathering and dissolved carbon dynamics to hydrological conditions in a typical karst river. *Scientific Reports*, *7*(January), 1–9. https://doi.org/10.1038/srep4294410.1038/srep42944

Zhou, Y., Xu, J. F., Yin, W., Ai, L., Fang, N. F., Tan, W. F., et al. (2017). Hydrological and environmental controls of the stream nitrate concentration and flux in a small agricultural watershed. *Journal of Hydrology*, *545*, 355–366. https://doi.org/10.1016/j.jhydrol.2016.12.015

Zuecco, G., Penna, D., Borga, M., & van Meerveld, H. J. (2016). A versatile index to characterize hysteresis between hydrological variables at the runoff event timescale. *Hydrological Processes*, *30*(9), 1449–1466. https://doi.org/10.1002/hyp.10681

References From the Supporting Information

Lyne, V., & Hollick, M. (1979). Stochastic time-variable rainfall-runoff modelling. In: *Proceedings of the hydrology and water resources symposium* (pp. 89–92).

Parde, M. (1933). *Fleuves et Rivieres*. Colin.